SEDIMENTOLOGY OF THE TOLEDO FORMATION, BELIZE BASIN, CENTRAL AMERICA

By

Jason Dominic Fisher

A thesis submitted to the Graduate Faculty of
Auburn University
In partial fulfillment of the
requirements for the Degree of
Master of Science

Auburn, Alabama
May 07, 2017

Keywords: Belize, submarine fan facies,
hydrocarbon, geochemistry

Approved by
David King, Jr., Chair, Professor of Geology
Willis Hames, Professor of Geology
Charles Savrda, Professor of Geology

Abstract

SEDIMENTOLOGY OF THE TOLEDO FORMATION, BELIZE BASIN,

CENTRAL AMERICA

Jason Dominic Fisher

The Toledo formation represents a profound shift from carbonate-dominated to clastic-dominated deposition within the Belize basin following the Late Cretaceous collision of the Maya and Chortis blocks (of the North American and Caribbean plates). The present study characterizes the lithological and petrographic makeup, depositional environments and provenance of the Toledo formation. The sedimentological characteristics can be described according to submarine-fan facies model put forward by Mutti and Ricci-Lucchi (their Facies A-G). Facies characteristics and associations indicate outer fan/depositional lobe, mid-fan, submarine canyon, and shelf depositional environments encompassing channel, depositional lobe, and sheet architectural elements.

Petrographic analysis of the shelf-derived carbonate samples from the Toledo formation show a dominance of shallow-water benthics. These units are interpreted as slope deposits based on models described by Schlager. Sandstones are the dominant lithology and are identified as immature lithic arenites based on petrographic analysis.

Plots of detrital modes of the sandstones on ternary diagrams identify a recycled orogen provenance related to the collision of the North American and Caribbean tectonic plates.

The Toledo formation has demonstrated economic potential for hydrocarbon and groundwater resources. Petrographic results suggest that the formation is best suited as a seal for the Cretaceous hydrocarbon resources, and for groundwater resources. Preliminary geochemical analysis revealed that the total organic-carbon (TOC) content of the Toledo formation rocks range from 0.2 to 1.86 wt% with an average of TOC value of 0.85 wt% indicating fair to poor source-rock potential. These contain mostly type IV with minor type III kerogen indicating terrigenous organic matter derived from woody plants, with little to no hydrocarbon-generating potential. Based on T_{max} (430 to 439 °C) and PI values, the studied samples are immature to early mature in terms of hydrocarbon generation.

Acknowledgments

This research was supported in part by funding from the Big Creek Group, Independence, Belize, The Geological Society of America, Gulf Coast Association of Geological Societies, American Association of Petroleum Geologists, and the Waters-Folse research grants. I would especially like to express my gratitude to Dr. David King, professor and friend, who challenged me to perform my best. A special thank you to my beloved wife Candace, words cannot express how grateful I am for all the sacrifices that she has made on my behalf. To my beloved daughter Ryleigh, dida is coming home. In addition I thank colleagues from Belize for accompanying him into the field area.

Table of Contents

Table of Figures

List of Tables

1. INTRODUCTION

The Belize basin consists of a thick sequence of Late Paleozoic to Quaternary rocks. Successions within the basin, particularly Upper Cretaceous to Quaternary deposits, are exposed along major highways in southern Belize. The informal[1] Toledo formation is a ~3000 m (~10,000 ft) thick unit representing a shift from carbonate-dominated sedimentation during Cretaceous to clastic-dominated deposition during Paleogene. During its history, the basin experienced active tectonism due to the collision (transform) of the North American and Caribbean Plates.

Exploratory wells in southern Belize have demonstrated the potential for hydrocarbons both onshore and offshore in the Belize basin. The Toledo formation has been identified as a potential source and seal for Cretaceous reservoirs in the Belize basin (Sanchez-Barreda, 1990). The formation also is part of the Upper Cretaceous to

[1] All stratigraphic units in Belize are informal. Both the International Stratigraphic Guide, 2nd edition (Salvador, 1994), and the North American Stratigraphic Code (NACSN, 2005) state that formal units must be published in a recognized scientific medium and must include a statement of intent to designate that formal unit. On both of these points, all stratigraphic units in Belize fail to qualify as formal units. All stratigraphic units in Belize are "provisional informal names," as discussed in the International Stratigraphic Guide, 2nd edition (Salvador, 1994). Therefore, we use the lower case "f" on formations to make clear the continued informal status of these units.

Paleogene aquifer system in southern Belize, providing freshwater for a large percentage of the population (GEOMEDIA, 2014). Despite its importance, the unit has not been formalized and is understudied. The goal of this study is to better understand the sedimentology of the Toledo formation.

Geology of the Study Area

Belize is located on the southern edge of the Yucatán Peninsula, where it forms part of the Maya tectonic block, which includes the Yucatán Peninsula and the northern section of Guatemala (Lallemant and Gordon, 1999). Based on surface mapping and geophysical surveys, Belize is divided into two distinct onshore regions: northern Belize, with dominant low-frequency geophysical anomalies, and southern Belize, with dominant high-frequency anomalies (Ramanathan and Garcia, 1991).

The southern basin, the Belize basin, is a Late Paleozoic to Quaternary feature. The Belize basin is the eastern extension of the Chapayal basin in Guatemala, located south of the La Libertad Arch and Maya Mountains (Vinson, 1962). The boundary between the North American and Caribbean plates is known as the Motagua-Polochic fault system, which passes just south of Belize near the southern limit of the Belize Basin (Ramanathan and Garcia, 1991; Leroy et al., 2000; Figure 1). Three factors have contributed significantly to the tectonic activity in the region; the close proximity of the Motagua-Polochic fault system, the post-Mesozoic closure of the sea floor between the south-moving Yucatán block and the Mexican crustal region, and the advent of a Cayman trough-related transform fault in the area of the Belize basin (Leroy et al., 2000; Kim et al., 2011).

The Toledo formation is a thick series of clastic facies that occurs in Belize. In Belize and Guatemala, The Toledo formed adjacent to the Maya Mountains along the northern margin of the Belize basin (Bryson, 1975; Fisher and King, 2015). The Toledo formation ranges in thickness from 30 to 3000 m (100 to 10,000 ft) in Belize, and overlies the 'KT' boundary interval and/or the Upper Cretaceous Campur formation (informal) and is overlain by the informal Belize formation (Fig. 2). A disconformity separates the Toledo and Belize formations (Petersen et al 2012).

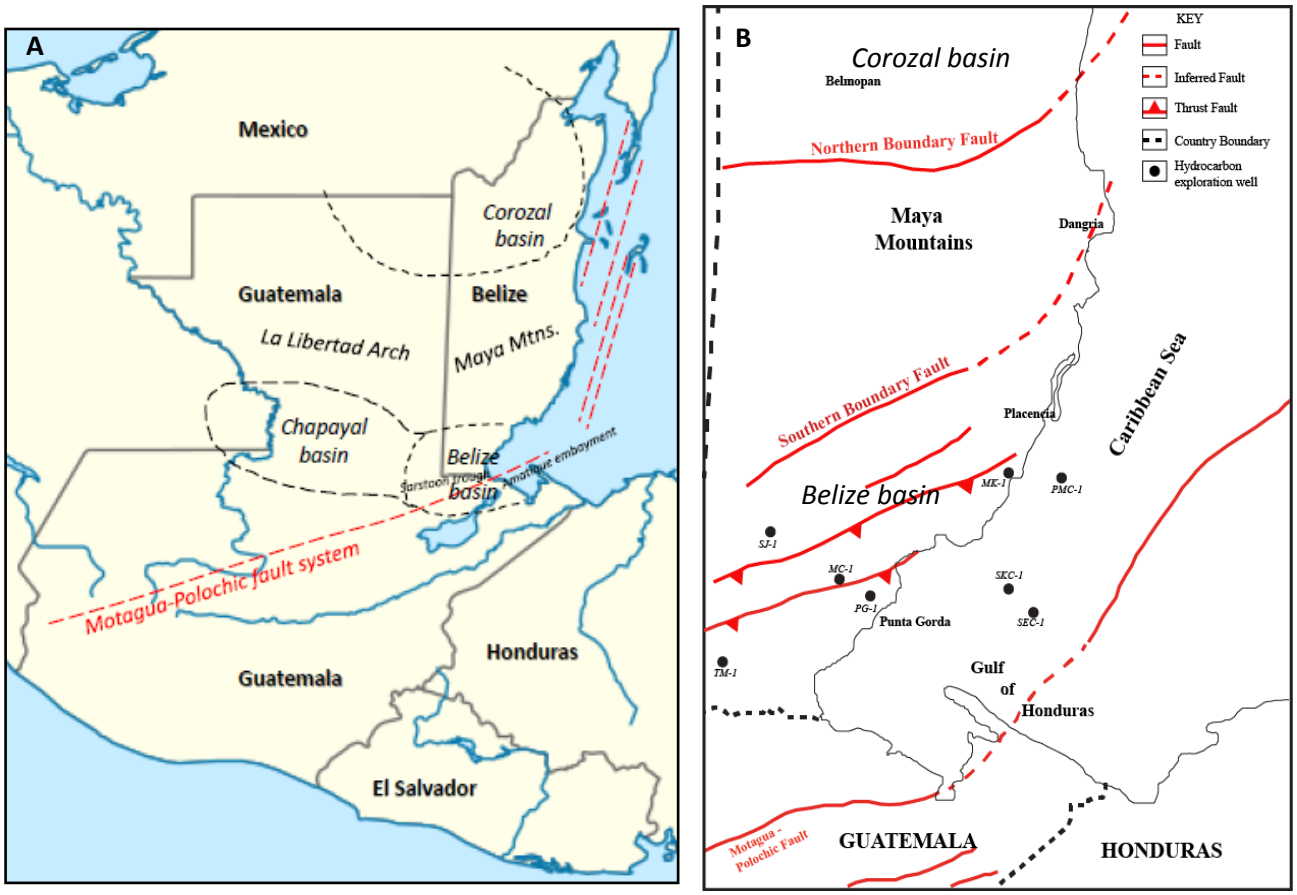

Figure 1-1: A) Regional map of Central America showing major features. B) Close up of Belize showing structural features of Belize and hydrocarbon exploration wells Temash 1 (TM-1), San Juan-1 (SJ-1), Machaca-1 (MC-1), Palmetto Caye -1(PMC-1), Punta Gorda -1(PG-1), Monkey River-1 (MK-1), Seal Caye-1 (SEC-1) and South Garbutt Caye-1(SKC-1). Modified from Cornec, 2003

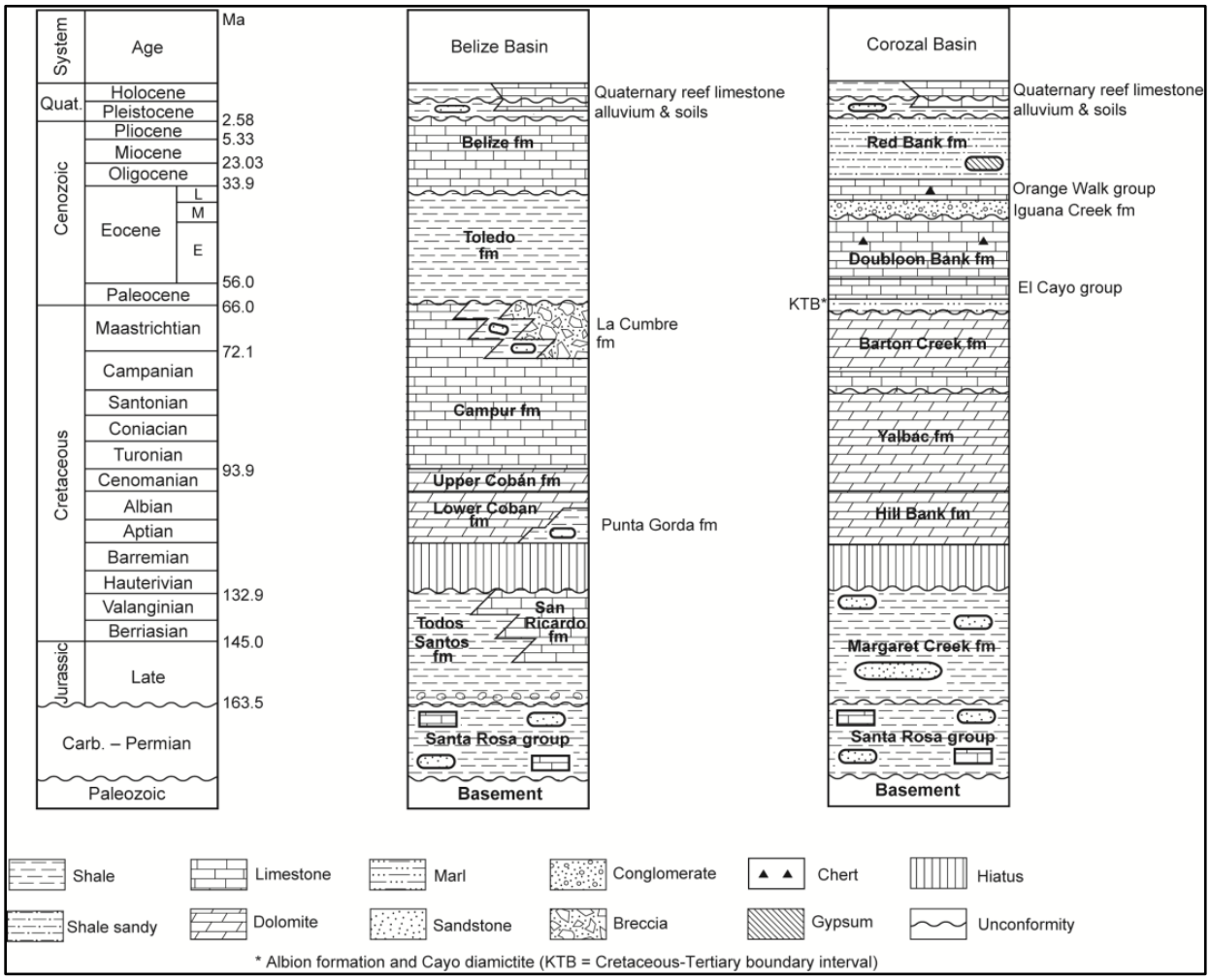

Figure 1-2: Stratigraphy of the basins of Belize. Basins can be seen on the map in Figure 1B (modified from Petersen et al., 2012).

Previous Work

Previous work on the informal Toledo formation generally focused on the descriptions of the Toledo formation in the neighboring south Petén basin (Guatemala) and to a lesser extent the Toledo formation of Belize basin. Research that focuses more on Guatemalan stratigraphy, but pertinent to the Belize basin, includes work by Ower (1928), Dixon (1956), Vinson (1962), and Bryson (1975). Recent contributions to the stratigraphy of the Toledo formation in Belize includes work by Ramanathan (1985, 1990), Ramanathan and Garcia (1991), Keller et al. (2003), and Schafhauser et al. (2003). All of these papers provide background stratigraphic framework and a general guide to the tectonic relations in the area. Schafhauser et al. (2003) refer to the Toledo formation and related Sepur Formation of Guatemala as thick "flysch sequences."

Stratigraphy

The Toledo formation is an unconformity-bounded unit that is underlain by the 'KT' boundary interval and/or Upper Cretaceous section (namely two informal units, the Campur formation and La Cumbre carbonate breccia; Fig. 2). Keller et al. (2003) referred to the 'KT' boundary interval as part of the "Sepur/Toledo formation." An unconformity occurs at the base of both the Toledo and 'KT' boundary interval, which may be the rationale for the nomenclature of Keller et al. (2003). Keller et al. (2003) assigned all rocks below the Toledo and the 'KT' boundary interval to uppermost Maastrichtian. A disconformity separates the Toledo from the overlying Belize formation. This stratigraphic break is near the Eocene-Oligocene boundary.

Lithology

Lithological descriptions of a few outcrops of the Toledo formation in southern Belize were completed by Ower (1928), Dixon (1956), Vinson (1962), Bryson (1975), Ramanathan and Garcia (1991) and Fisher and King (2015). Ower (1928) introduced the designation “Toledo Series” and described the formation as a thick series of clastics including shales, mudstones, calcareous sandstone and limestones. Dixon (1956) noted that the entire Toledo “series” weathers characteristically to a “rich chocolate brown color” on account of the ferruginous and organic materials contained in the fine clastic sediment. Since Bryson’s (1975) report, however, the Toledo has been known as a formation.

Dixon (1956) described the Toledo overall as a “series of thin bedded shales and mudstones with blue calcareous sandstones.” Bryson (1975) identified the Toledo as a “thinly interbedded fine detrital sandstone and mudstone with hard, dark, calcareous sandstone in the lower part.” Bryson (1975) noted that the Toledo formation may be compared with the Guatemalan Sepur Formation with the only significant difference being the occurrence of thick calcareous sandstones in the lower section of the Toledo. The lower sandstones of the Toledo contain mafic grains that are considered characteristic and distinctive to those beds (Vinson, 1962; Bryson, 1975). Fisher and King (2015) identified three major facies in the Toledo formation: interbedded sandstone-mudstone, sandstone, and conglomerate-dominated.

A type section for the Toledo formation has not been designated. However, Vinson (1962) suggested a Toledo type section in the Toledo District of British Honduras (Belize); however, it was never clearly defined. A reference section in

southeastern Petén basin of Guatemala was proposed by Vinson (1962), wherein repetitious interbedded claystones and siltstones with lesser sandstone, calcarenites, calcisiltites, and limestone conglomerates are exposed. However, this would pertain more to the equivalent Sepur Formation than to the Toledo. In Belize, two major outcrops have been described by Dixon (1956) occurring in the regions of the faults in Figure 1B. However, these outcrops were not clearly located.

Vinson (1962) describes the Toledo formation in Guatemala as having uniform bedding, generally between 2.5 and 7.5 cm (1 to 3 in) thick. Thin to medium beds of "whitish tan" calcarenites and calcisiltites, which are generally poorly sorted and contain igneous and limestone grains and chert, are exposed in several outcrops. Thin lenticular limestone and limestone-chert conglomerate beds (with fragments of limestone, chert, and igneous clasts) occur less commonly. In general, the coarser beds are more common in the basal part of the Toledo formation exposed in Guatemala. Because of the complex structure of the region and the formation's great thickness, it is unlikely that a complete section of the formation is exposed anywhere in Guatemala or Belize.

The dip of the Toledo formation is toward the south. Dixon (1956) states that Cretaceous and younger strata situated south of the Maya Mountains and north of the San Antonio fault dip southward at low angles. South of the Moho River fault, rocks display similar low dips. However, between the San Antonio and Moho River faults, the structural dips are much steeper. In general, an east-west to northeast-southwest strike prevails in the Belize basin and in the Toledo formation in particular (Vinson, 1962). Unpublished reports on a deep exploration well in the Belize basin, Temash-1 (TM-1),

present dips ranging from 30° to subvertical from core analysis and up to 50° from dip-meter analysis. This well is southwest of the features mentioned above (Fig. 1B).

Biostratigraphy and paleoenvironment

Studies of biostratigraphy, paleoecology, and paleogeography related to the Toledo formation and associated stratigraphic units have been done by Ower (1928), Bronniman and Macaulay (in Dixon, 1956), Ramanathan (1985, 1990), Ramanathan and Garcia (1991), and Keller et al. (2003). Ower (1928) thought the Toledo to be Miocene, but it was later identified as early Eocene by Bronniman and Macaulay (in Dixon, 1956). A 30-cm-thick limestone layer, located 2.4 km north of the village of San Antonio in the Toledo District, contains a foraminiferal assemblage of *Globorotalia*, *Truncorotalia*, *Globigerina*, *Discocyclina*, and *Lepidocyclina*(?) (Bronniman and Macaulay, in Dixon, 1956). Ramanathan (1985, 1990) and Ramanathan and Garcia (1991) conducted a series of detailed micropaleontological studies of the cuttings from a select group of wells drilled across Belize (both in the Corozal and Belize basins). Unpublished studies on samples of the Toledo formation from wells in the Belize basin suggest that the foraminifera are late Campanian to Early Paleogene.

Keller et al. (2003) worked on the spherule deposits in Cretaceous-Paleogene ('KT' boundary) sediments of Belize and Guatemala. They identified the contact between the Toledo and the underlying Cretaceous Campur formation. At this contact, an assemblage including *Globoconusa daubjergenesis*, *Globigerina* (*E.) eobulloides*, *Pyrulina extensa*, *Parvularugoglobigerina eugibina*, and *Guembelitria cretacea* was

used to identify its age as Paleocene. Based on this, the formation is now considered to be a Paleogene deposit.

Foraminiferal assemblages in the Toledo formation suggest a variety of environments from lagoonal to bathyal (Ramanathan, 1985, 1990), and the dominance of planktic foraminifera suggests relatively oxygen-deficient bottom conditions (Ramanathan and Garcia, 1991). A synthesis of Campanian paleogeography suggests the development of a deep marine trough in the Belize basin (Ramanathan and Garcia, 1991; Schafhauser et al., 2003). Based on the facies identified by Fisher and King (2015), the depositional environment is interpreted as a submarine-fan complex with channelized and non-channelized associations.

Economic resources

A groundwater-resource assessment of southern Belize (GEOMEDIA, 2014) identified a distinct multilayered sedimentary aquifer system in the Belize basin which holds large reserves of groundwater. Quaternary to Holocene sediments make up a shallow aquifer system, and Late Cretaceous to Paleocene rocks make up a deeper aquifer system. In this deeper system, coarser strata of the Toledo formation, particularly the calcareous sandstones units are water bearing, whereas mudstones/clays act as aquitards. This assessment was conducted just northeast of the exposures of the Toledo in close proximity to the village of Golden Stream. Unpublished drilling reports from the Ministry of Rural Development in Belize, identify aquifers ranging in depths from 20-100 m (65 to 328 ft) in the Toledo formation and Quaternary deposits in the region. Local aquifers have also been documented in

hydrocarbon exploration wells particularly in the San Juan and Monkey River well logs (GEOMEDIA, 2014).

The Belize basin also has been the site of numerous hydrocarbon exploration wells, the most recent being Temash #2, drilled by US Capital Energy in 2014. Including this well, a total of 8 wells has been drilled onshore within the Belize basin, and of these, four had petroleum shows (Geology and Petroleum Department, 2014). The Toledo formation has been drilled in at least 6 of these 8 onshore wells. Oil seeps are known to occur within the basin and have been identified in sandstones of the Toledo in Punta Gorda (Bryson, 1975), and in limestones of the Cretaceous Cobán Formation, around the town of Punta Gorda (Petersen et al., 2012). Sanchez-Barreda (1990) stated that the Toledo formation has demonstrated hydrocarbon source and seal potential.

Objectives

The objectives of the research are: (1) lithofacies and environmental analysis of the Toledo formation, which is thought to be a flysch type/submarine-fan deposit in Belize; (2) petrographic analysis (compositional) of sandstones and carbonates to determine diagenetic history and provenance; and (3) preliminary organic geochemical analysis to assess the formation's hydrocarbon source potential.

This thesis follows a manuscript format and comprises three papers written to satisfy the format of the target journals. The first paper, "Paleogene Submarine Fan Deposits in Southern Belize," which was published in the Gulf Coast Association of Geological Society's *Transactions* (2016, volume 66, p. 181-195) is a detailed synthesis of the submarine fan facies of the Toledo formation. The second paper, "Petrofacies

analysis of the Toledo formation: implications for carbonate deposition and tectonic provenance," is to be submitted to *Journal of South American Earth Sciences*. This paper provides a petrographic analysis of carbonates and sandstones of the Toledo formation and provides a provenance analysis based on detrital modes from the sandstones. The third and final paper, "Preliminary source rock evaluation of the Toledo formation, southern Belize," is to be submitted to *Petroleum Geology*. This paper assesses the source-rock potential of the formation using standard geochemical techniques.

References

Bryson, R.S., 1975, Regional Geology, Petroleum and Mineral Potential of southern Belize: Denver, Colorado, Anschutz Overseas Corporation, 22 p.

Cornec, J.H., 2003, Geology map of Belize: Belmopan, Belize, Geology and Petroleum Office, scale 1:750,000.

Dixon, C.G., 1956, Geology of Southern British Honduras with notes on adjacent areas: Belize City, British Honduras, Government Printing Office, p. 1-85.

Fisher, J. D., and King, Jr., D. T., 2015, Stratigraphy of the Toledo formation, Belize basin, southern Belize: Gulf Coast Association of Geological Societies Transactions, v. 65, p. 107–123

Geology and Petroleum Department, Ministry of Energy, Science, Technology and Public Utilities, Government of Belize, 2014, Geophysical Surveys and wells drilled in Belize 2000-2014, map.

GEOMEDIA 2014, Assessment of Groundwater Resources in the southern Coastal Water Province of Belize referred to as Savannah Groundwater Province, unpublished, final report: United Nations Development Programme (UNDP), Belmopan, Belize, GCCA/PS/2013/14, p.136.

Keller, G., Stinnesbeck, W., Adatte, T., Holland, B., Stüben, D., Harting, M., de Leon, C., and de la Cruz, J., 2003, Spherule deposits in Cretaceous-Tertiary boundary sediments in Belize and Guatemala: Journal of the Geological Society, v. 160, p. 783-795.

Kim, Y., Clayton, R.W., Keppie, C., 2011, Evidence of a collision between the Yucatán block and Mexico during Miocene: Geophysical Journal International, v. 187, p. 989-1000.

Lallement, H.G., and Gordon M.B., 1999, Deformation History of Roatán Island: Implications for the Origin of the Tela basin (Honduras), in Mann, P. (Series Editor: K.J. Hsü), Caribbean basins: Sedimentary basins of the World, 4, p.197-218.

Leroy, S., Mauffret, A., Patriat, P., and Mercier de Lépinay, B., 2000, An alternative interpretation of the Cayman trough evolution from re-identification of magnetic anomalies: Geophysical Journal International, v. 141, p. 538–557.

Ower, L.H., 1928, Geology of British Honduras: Journal of Geology, v. 36, p. 494-509.

Petersen, H.I., Holland, B., Nytoft, H.P., Cho, A., Piasecki, S., de la Cruz, J., and Cornec, J.H., 2012, Geochemistry of crude oils, seepage oils and source rocks from Belize and Guatemala: indications of carbonate-sourced petroleum systems: Journal of Petroleum Geology, v. 35, p.127-163.

Ramanathan, R., 1985, Foraminiferal micropaleontological report on Dangriga well-1, offshore Belize: Belmopan, Belize, Geology and Petroleum Office, UNDP/BZE/ 83/001, 13 p.

Ramanathan, R., 1990, Foraminiferal micropaleontological report on Belize: Belmopan, Belize, Geology and Petroleum Office, UNDP/BZE/ 87/003, 23 p.

Ramanthan, R., and Garcia, E., 1991, Cretaceous paleogeography, foraminiferal biostratigraphy, and paleoecology of Belize basin: Transactions of the 2nd Geological Conference of the Geological Society of Trinidad and Tobago: Port of Spain, Trinidad, p. 203-211.

Sanchez-Barreda, L, A., 1990, Why wells have failed in southern Belize: Oil and Gas Journal, August, p. 97-103.

Schafhauser, A., Stinnesbeck, W., Holland, B., Adatte, T., and Remane, J., 2003, Lower Cretaceous Pelagic Limestones in Southern Belize: Proto-Caribbean deposits on the Southeastern Maya Block. *In* Bartolini, C. R.T. Buffler, and J. Blickwede (eds.), The Circum-Gulf of Mexico and the Caribbean: Hydrocarbon habitats, basin formation, and plate tectonics: Tulsa, Oklahoma: American Association of Petroleum Geologists Memoir 79, p. 624-637.

2. PALEOGENE SUBMARINE FAN DEPOSITS IN SOUTHERN BELIZE

Jason D. Fisher and David T. King, Jr.

Published in the *Gulf Coast Association of Geological Societies Transactions*, 2016, v. 66, p. 181–195.

Abstract

Deposition of the Toledo formation represents a distinctive shift from a carbonate-dominated basin to a clastic-dominated basin following the collision of the Maya and Chortis blocks of the North American and Caribbean plates, respectively, near the end of Late Cretaceous. We analyzed the sedimentology and stratigraphic record of the Toledo deep-water sequence along two major outcrop transects in southern Belize. These transects are dominated by marine deep-water facies successions, both indicating proximal provenance. Sedimentological characteristics of the Toledo are best described according to submarine fan facies model discussed in papers by E. Mutti and F. Ricci-Lucchi, specifically their faces A-G. Facies associations along the southern highway pertain to the mid-fan depositional environment and its associated subenvironments, particularly interchannel fringe areas encompassing channel, depositional lobe, and sheet architectural elements.

Introduction

The Belize basin is located south of the Maya Mountains in southern Belize (between the Southern boundary fault and the Motagua-Polochic fault system; Fig. 2-1A) and the eastward extension of the Chapayal basin of adjacent Guatemala (Vinson, 1962). On the southern limit of the Belize basin lies the Motagua-Polochic fault system, an Eocene left-lateral strike-slip fault system, which is related to a late stage of collision between of the North American and Caribbean plates (Purdy et al., 2003). The Cenozoic section of the Belize basin (i.e., the Toledo formation) is exposed continuously along parts of the Southern highway and Mile 14 highway in southern Belize (Figure 2-1B) providing a unique opportunity to study clastic sedimentation in this part of the Belize basin. The entire Cenozoic section consists largely of the clastic Toledo formation, which reaches thicknesses of up to 3000 m as observed in exploratory wells. This thick sequence of interbedded sandstones, mudstones, conglomerates, and limestones unconformably overlies Upper Cretaceous carbonate units (mainly the Campur and La Cumbre formations, and/or 'KT' boundary ejecta deposits).

Previously, we interpreted that the Toledo complex of submarine fans extends eastward from the Belize-Guatemala border along the southern Maya Mountains and offshore into the adjacent western portion of the Caribbean Sea (Fisher and King, 2015; Fisher et al., 2016). Toledo submarine fans probably developed in response to the collision of North American and Caribbean plates and related tectonism (Purdy et al., 2003). Calcareous nannofossil biostratigraphy identifies a middle Paleocene (Selandian) age for outcrops of the Toledo formation in this study (Fisher et al., 2016). This age postdates the convergence of the Late Cretaceous North American and

Caribbean plates and predates tectonic activity in the Eocene Motagua-Polochic fault zone.

This paper follows up on recent studies by Fisher and King (2015), further detailing the submarine fan facies of the Toledo and their associated subenvironments. The present paper extends work on the Toledo formation over a wider area and in more sedimentological detail. In this study exposures of the Toledo formation along the Southern Highway and Mile 14 Highway were logged. Emphasis was placed on lithology, texture, physical and biogenic sedimentary structures.

Submarine Fans and their Facies

Submarine fans have been studied for the past 65 years, resulting in several classification schemes (see discussion in Shanmugan, 2000). Of particular interest, Mutti and Ricci Lucchi (1972), Walker and Mutti (1973), and Ricci Lucchi (1975a, 1975b) have identified seven lithofacies categories in submarine fan settings, facies A through G. These facies descriptions incorporate physical characteristics of grain size, bed thickness, sand-to-shale ratio, bedding continuity, and associated structures. Submarine fan deposits are generally referred to as turbidities deposits, although not all submarine fan sedimentation is by the process of turbidity currents (Shanmugam, 2000). Other processes include hemipelagic sedimentation, contourite deposition, mass transport (slide/slump processes), and debrite-emplacement processes (Shanmugam, 2000; Stow and Mayall, 2000). Several workers (Reading and Richards, 1994; Stow and Mayall, 2000; Sprague et al., 2002a, 2002b) have attempted to modify and refine the submarine fan facies models of the authors cited above. For example,

Stow and Mayall (2000) characterizing the fundamental building blocks, herein referred to as architectural elements. Submarine fan deposits exhibit a predictable arrangement of architectural elements that typically vary between submarine fan types. Architectural elements are components of the depositional system that are products of the processes operating within subenvironments of the submarine fan.

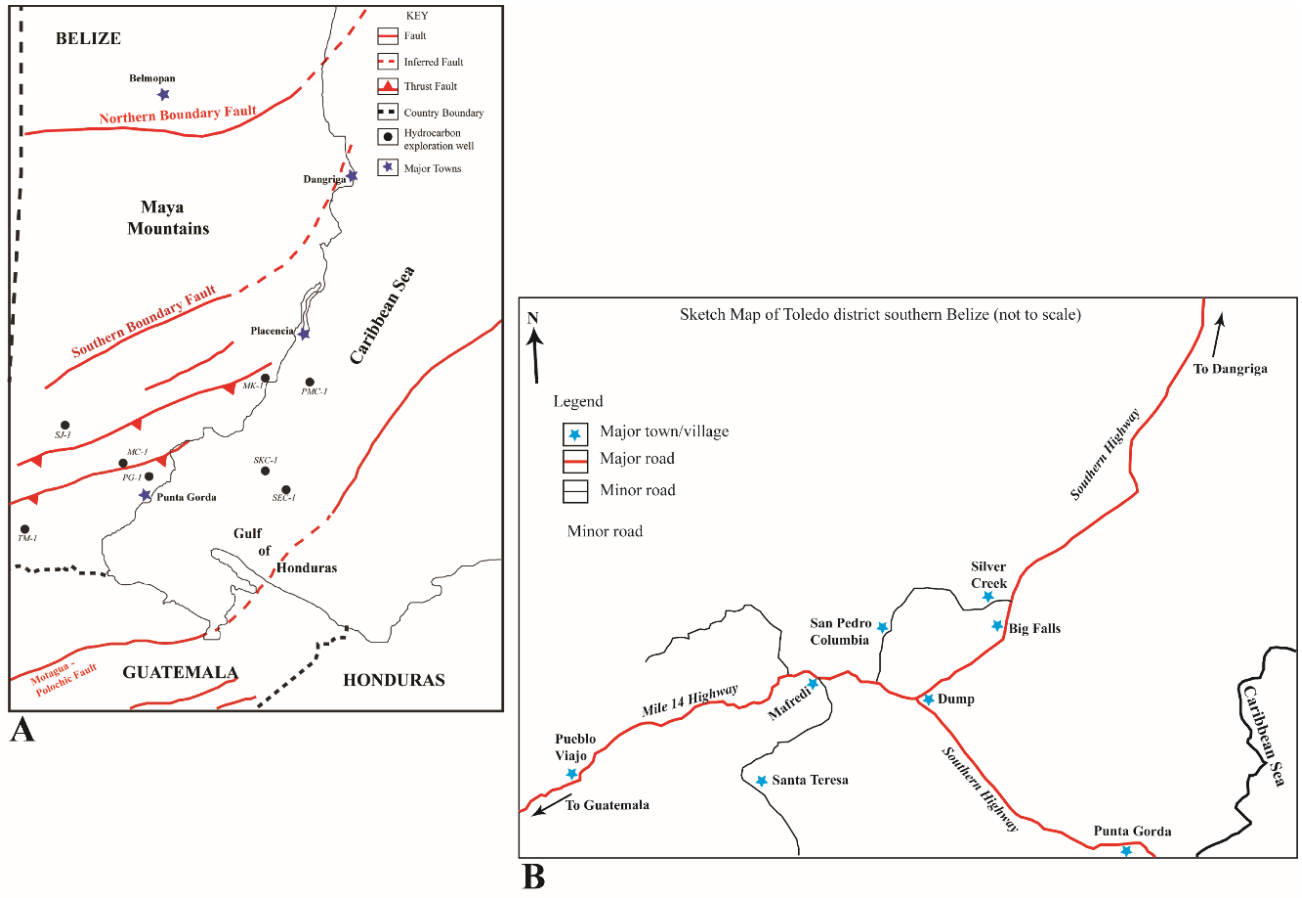

Figure 2-1: Simplified structural map of central and southern Belize showing key faults, major towns, and locations of exploratory wells drilled (modified after Purdy et al., 2003); (B) Sketch map of southern Belize showing highways, roads, and key towns. The study area follows the southern highway to Dump and from Dump to Pueblo Viajo to the west.

The principal architectural elements are channel, levee and overbank, depositional lobes, sheets and drapes, and chaotic mounds (Reading and Richards, 1994; Stow and Mayall, 2000; Sprague et al. 2002a, 2002b). These elements occur at a range of scales and within varying facies associations.

Fisher and King (2015) identified three main submarine fan facies in the Toledo formation: interbedded sandstone-mudstone, sandstone, and conglomerate-dominated facies. In this study, submarine fan facies will be described using the criteria of standard facies models for submarine fan deposits (Table 2-1), while attempting to classify the architectural elements of the system at outcrop scale.

Toledo Submarine Fan Facies

Facies analysis allowed the definition of seven main facies that will be hereby described and interpreted based on their spatial and genetic relationship.

Table 2-1: Simplified facies classification after Mutti and Ricci-Lucchi (1972, 1975), Walker and Mutti (1973), and Ricci-Lucchi (1975a).

Facies	**Facies Description**
Facies A	Coarse-grained conglomerate and pebbly sandstone (no Bouma sequences)
Facies B	Medium- to coarse-grained massive sandstone (no Bouma sequences)
Facies C	Interbedded sandstone and mudstone; proximal turbidites (no Bouma sequences?)
Facies D	Interbedded mudstone and sandstone; distal turbidites
Facies E	Interbedded sandstone and mudstone; overbank and inter-channel deposits
Facies F	Chaotic deposits (no Bouma sequences)
Facies G	Mudstone, pelagic, and hemipelagic deposits, cherts, and marlstones (no Bouma sequences)

Facies A

This facies has been described as either ‘disorganized’ or ‘organized’ by Walker and Mutti (1973) and Mutti and Ricci-Lucchi (1975). Facies A consists of coarse-grained conglomerates (both clast- and matrix-supported) and medium to coarse-grained, pebbly sandstone (Figs. 2-2A to 2-2D). The conglomerates are polymictic; clasts include but are not limited to micritic limestone, dolomite, and a variety of volcanics. The clasts are generally cobble-sized, but include rare boulders. Number and sizes of clasts typically decrease upwards. The matrix is generally medium- to coarse-grained, calcareous grey sandstone. In the study area, only one occurrence of crudely laminated conglomerate is observed (Fig. 2-2C). The conglomerates are typically thick to massive, reaching 4 m. Generally, they are lenticular, with some

wedging, and show obvious scouring into underlying units. Gradational upper contacts characterize transitions from conglomerates to pebbly sandstones and sandstones of facies B (Fig. 2-2B).

The pebbly sandstone aspect of facies A is medium-grained calcareous sandstone, which contains pebbles and cobbles up to 10 cm (Fig. 2-2D). These pebbles are typically carbonate and volcanic rocks. Some units show an increase in pebble abundance from base to top. Pebbly sandstone beds are generally medium bedded, reaching thicknesses of 1.5 m. Although the beds commonly display gradational contacts (lower) with conglomerates, sharp contacts (upper) are observed with facies C (described later).

The depositional mechanisms for facies A are interpreted to be high-density turbulent currents resulting in mass deposition and freezing (see discussion in Lowe, 1982). Mulder and Alexander (2001) referred to these currents as concentrated density flows which includes sandy debris flow and grain flow described by Mutti and Ricchi-Lucchi (1972) and Lowe (1982). The classic Bouma sequence does not occur in this facies.

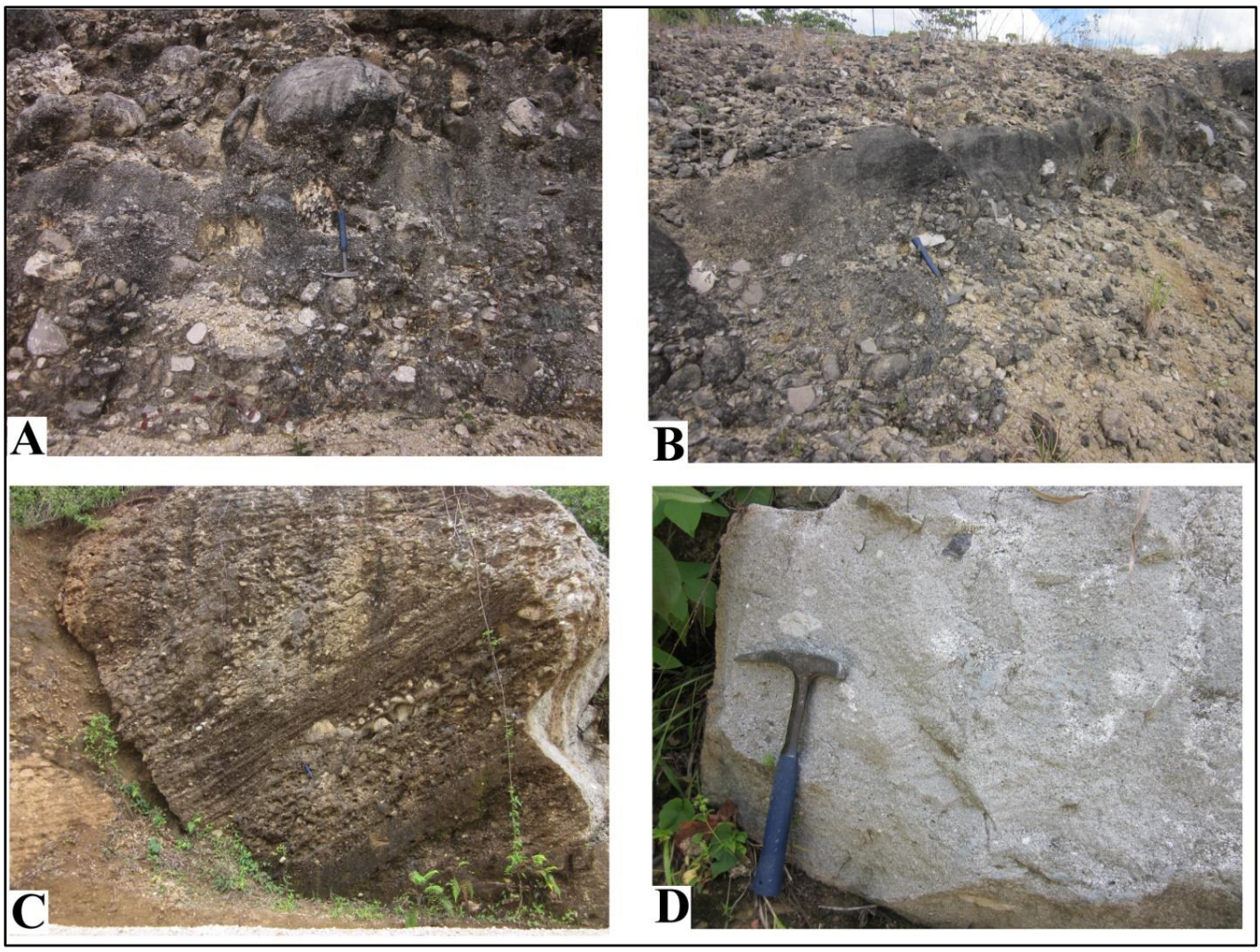

Figure 2-2: Facies A. (A) Pebble to boulder conglomerate; (B) conglomerate of facies A grading to sandstone of facies B; (C) crudely laminated conglomerate; and (D) pebbly sandstone.

Facies B

Facies B consists of micaceous, coarse- to medium-grained sandstone, which occurs in thick massive beds that have composite sequences (occurs with genetically related beds). Facies B sandstones typically reach thicknesses of 4.5 m in outcrops (Figs. 2-3A to 2-3C). Bases of these beds are generally erosional (scouring and channeling), and amalgamation of beds is common. Facies B depositional units have greater lateral continuity than those of facies A (Fig. 2-3C). Sole and tool marks are found on bases of beds of facies B, where they overlie facies C or E. Ripped-up and redeposited mud chips occur throughout facies B (Fig. 2-3B). Gradational contacts (lower) are observed between facies B and A, whereas sharp contacts (upper) are observed with other facies.

The depositional mechanisms for this facies likely include grain flow (hyper-concentrated density flow) and high-density turbulent flow (Mutti and Ricchi-Lucchi, 1972; Lowe, 1982; Mulder and Alexander, 2001). Combinations of these flow regimes maybe possible where facies B transitions into facies C (Mutti and Ricchi-Lucchi, 1972). The classic Bouma sequence does not occur in this facies.

Facies C

Facies C is characterized by fine- to coarse-grained sandstones, with common interbeds of mudstone. Sandstone beds are commonly 0.25 to 2.5 m thick and represent classical proximal turbidites characterized by grading to thin mudstone layers, alternating sequences with mudstone, and sole marks (Figs. 2-4A and 2-4B). Beds show little or no channelization as tops and bottoms of beds are parallel. Due to the

presence of thin interbeds of mud, sole marks and trace fossils tend to be well preserved. Sole marks are dominantly tool marks. Trace fossils are typically smooth and tubular, and are preserved in a variety of orientations. Sandstone-to-mudstone ratios are generally high.

These beds are interpreted to have been deposited primarily by classical turbulent flows but of a higher than normal density, resulting in mass deposition with the settling of large grains followed by possible reworking (see discussion of comparable units in Mutti and Ricchi-Lucchi, 1972). These high density turbulent flows have been classified as concentrated grain flows by Mulder and Alexander (2001). An immature Bouma sequence of structureless but ungraded sandstones Ta and homogenous mudstones Te, is evident in some beds of this facies.

Facies D

Facies D consists of thin, interbedded sandstones and mudstones. The mudstone is calcareous and generally silty. The sandstone is fine- to medium-grained and calcareous and there is a notable presence of organic matter in some outcrops. Beds are generally 5 to 40 cm thick, even, parallel, and persist laterally over many 10 s of meters. Localized wedging, shallow scour marks, slumping, and overturned beds (associated with soft sediment deformation and collapse of sediments or local tectonic disturbance) are common (Figs. 2-5A to 2-5D). Whereas sole marks are rare and developed on thicker beds, small burrows tend to be common (Fig. 2-5B). Sandstone-to-mudstone ratios are variable and are usually 1.0 or less. Beds in this facies may

contain the upper part of the classic Bouma sequence. Thick intervals of facies D strata are transitional (upward) with thin facies C beds (Fig. 2-4B).

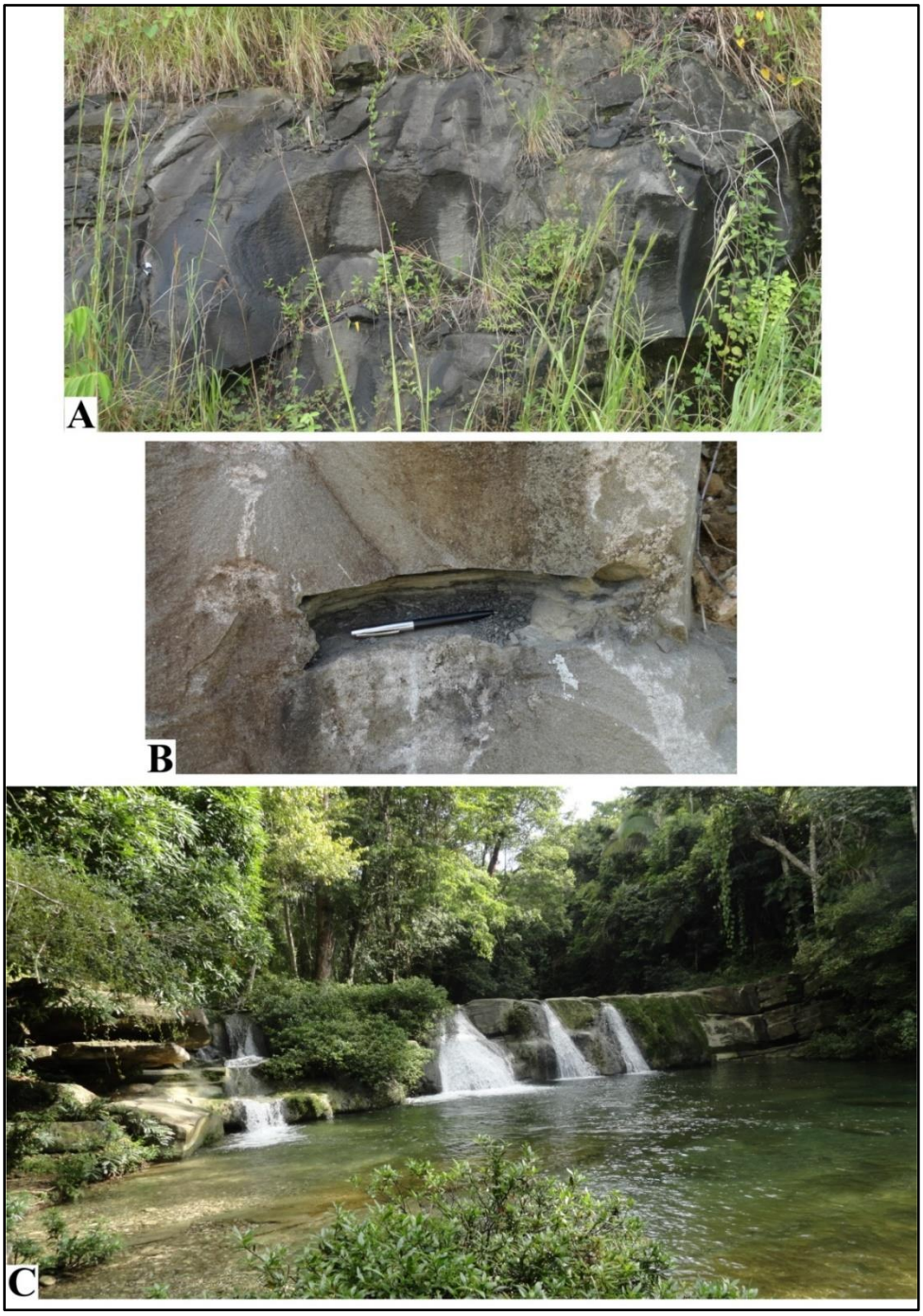

Figure 2-3: Facies B. (A) Massive sandstone; (B) mudstone rip-up clasts in massive sandstone; and (C) thick bedded sandstone.

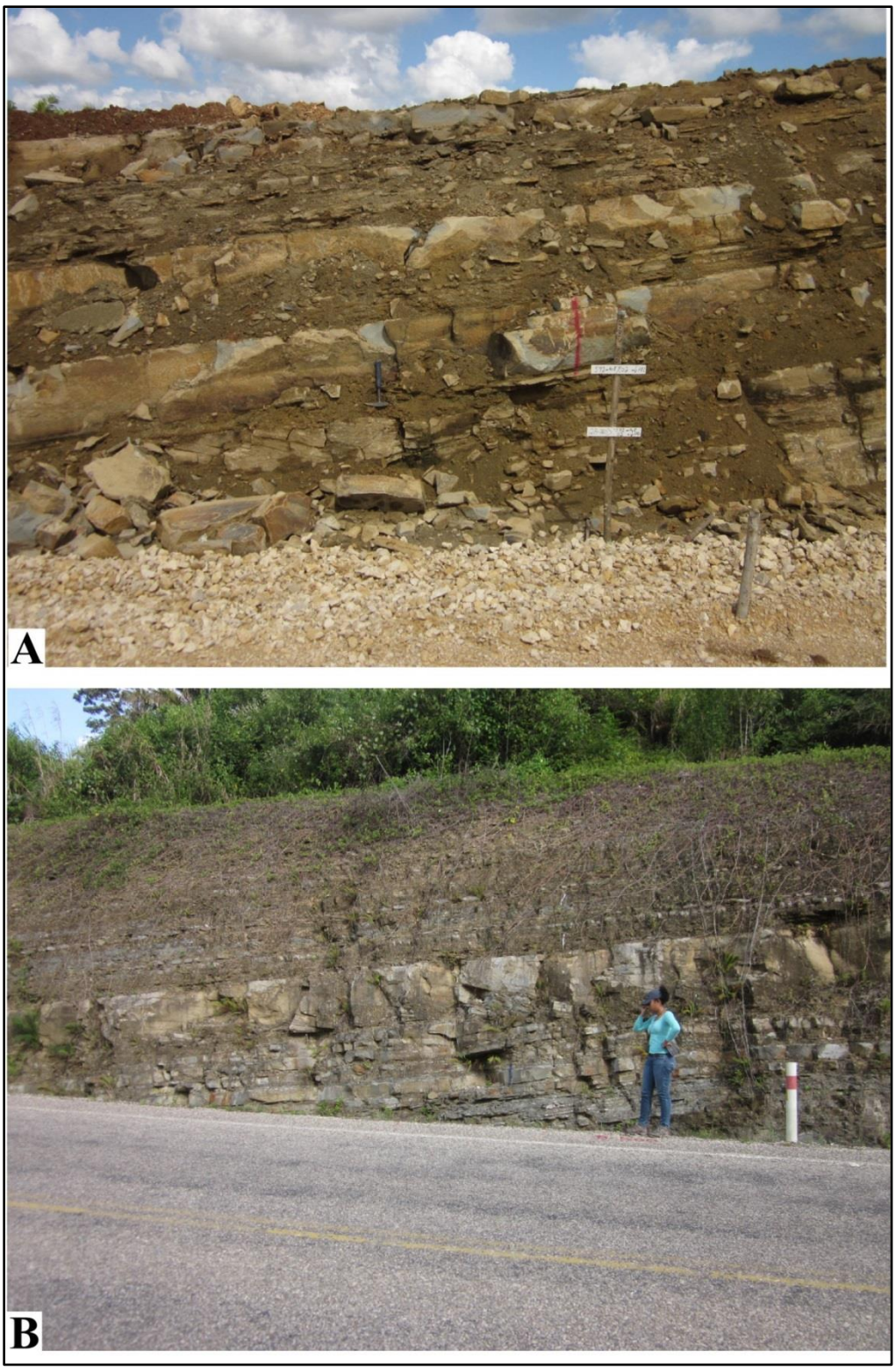

Figure 2-4: Facies C. (A & B) Two examples of interbedded sandstone and mudstone with transition to thin sandstone-mudstone of facies D.

The major depositional mechanism is interpreted to be a high to low density, mature turbidity currents wherein deposition occurs by traction and fallout from waning energies. (See discussion of comparable units in Mutti and Ricci-Lucchi, 1972.)

Facies E

Facies E deposits are similar to facies D in that they consist of interbedded sandstones and mudstones. However, facies E is differentiated by the occurrence of wavy and discontinuous bedding in the sandstone and by having a high to very high ratio of sandstone to mudstone (Fig. 2-6). This facies comprises only a very minor part of the Toledo formation in the study area. Beds of this facies fit the Bouma Tc division and are considered to reflect deposition by low density turbidity currents.

Facies F

Facies F includes remobilized deposits exhibiting mass slumping and localized re-sedimentation and may be referred to as chaotic and contorted deposits. There is some uncertainty in the assignment of a small number of pebbly mudstones and some of the conglomerates with regard to facies A versus facies F. In this paper, facies F includes most of the pebbly mudstones and the conglomerates (more properly called carbonate breccias) cropping out in the study area.

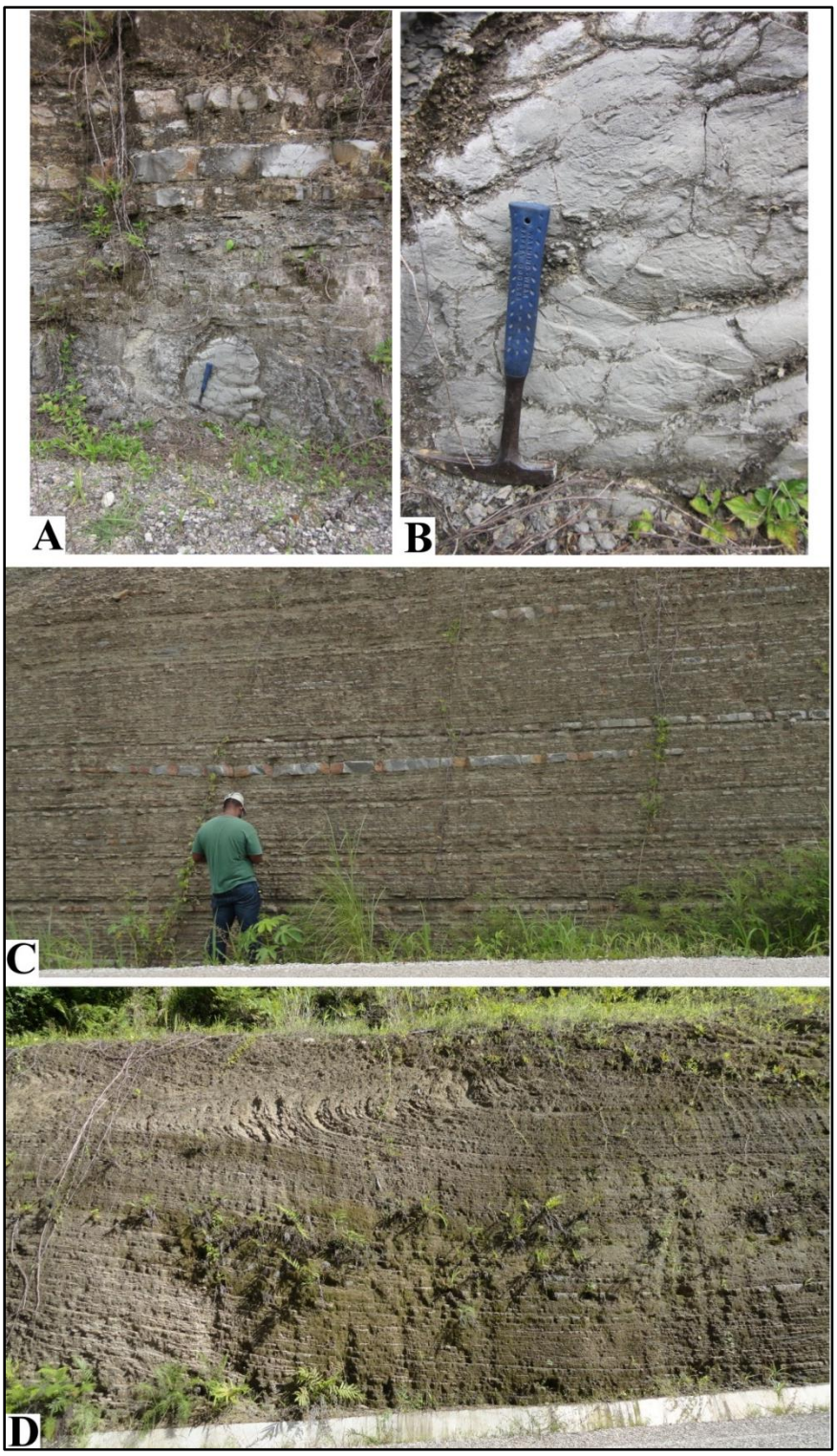

Figure 2-5: Facies D. (A & B) Two examples of overturned thin interbedded sandstone-mudstone showing tool marks at the base of overturned sandstone bed. (C) Thin interbedded strata of facies D showing shallow scouring. (D) Slumped facies D.

Figure 2-6: Facies E. Thin interbeds of sandstone-mudstone showing a high percentage of sandstone to mudstone ratio (center of photograph).

The pebbly mudstones contain subrounded to rounded clasts that are generally cobble-sized (Figs. 2-7A and 2-7B). Clasts are largely dominated by carbonates with minor volcanics. The clasts exhibit normal grading within the mudstone. These mudstones are characterized by abundant calcite filled fractures (Fig. 2-7B). Rare pebbly mudstone beds show an increase of silt content within the mudstone. The pebbly mudstones reach up to 3 m, are laterally extensive, and have sharp upper contacts with facies A and D. Rare discontinuous conglomerate beds are incorporated

into the pebbly mudstone creating sediment loading features such as flame structures (Fig. 2-7B).

The facies F conglomerate, or the Toledo carbonate breccia, are clast-supported and show reverse to normal grading (Fig. 2-7C). Only one unit was identified. The base of this depositional unit is marked by a 0.47 m thick (50 cm) carbonate gravel bed with fossil fragments and chert. The main breccia bed of this facies is 2.34 m thick is dominated by cobble- to boulder-sized clasts of limestone, and there are some sandstone/mudstone rip-up clasts. This main breccia bed grades upward into a 0.19 m thick skeletal wackestone-packstone.

We interpret the main depositional mechanisms for this facies as laminar debris flow and submarine sliding causing freezing and settling, resulting in inverse to normal grading, based on similar occurrences described by Shanmugan (2000).

Facies G

Facies G typically includes pelagic and hemipelagic mudstone deposits. Stow (1985) described this facies based on its composition, which included chalks, cherts, and marlstones. The descriptions of Stow (1985) as applied to the Toledo formation and carbonate facies—excluding breccias—are described here.

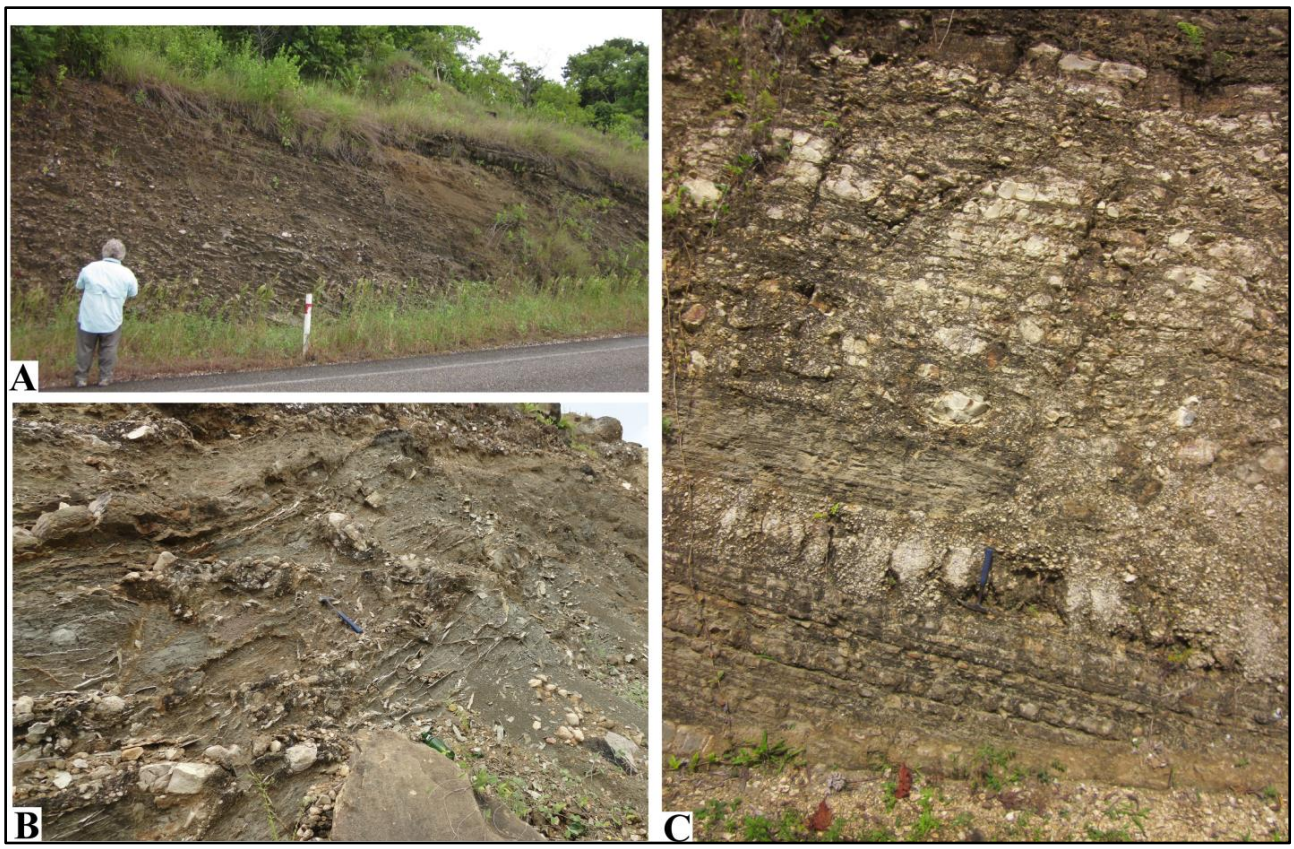

Figure 2-7: Facies F. (A) Pebbly mudstone of facies F transitioning to facies D; (B) pebbly mudstone showing fracture fills and floating discontinuous conglomerate within mudstone; and (C) carbonate breccia showing inverse to normal grading with rip-up clast of sandstone-mudstone.

Carbonate units of this facies include tan to buff skeletal wackestone-packstone (Fig. 2-8). These carbonate units are generally tabular and are laterally extensive. They range in thickness from 0.5 m to 1 m and are commonly associated with facies D. Vertical burrows are observed close to the bases of several units. Facies G is interpreted to have formed by intermediate currents or gravity-driven suspensions from a nearby carbonate shelf (see discussion in Mutti and Ricchi-Lucchi, 1972).

Figure 2-8: Facies G. Tan to buff wackestone-packstone of facies G, interbedded with facies D.

Submarine Fan Architectural elements

Submarine fans are divided into a number of architectural elements, which includes channel fills, levee and overbank, depositional lobes, sheets and drapes, and chaotic mounds (Reading and Richards, 1994; Stow and Mayall, 2000; Sprague et al., 2002a, 2002b). In the outcrops of the Toledo formation, we were able to clearly delineate channel fills, lobes, and sheet sands at outcrop scale. These are discussed briefly below.

Channel fills

Channel fills have been classified into four major types according to the classification of Mutti and Normark (1987; 1991). These types are: (A) erosional channel; (B1) depositional channel with coarse grained facies; (B2) depositional channel with alternating sandstone and mudstone beds; and (C) mixed channels (Fig. 2-9A). All channels types with the exception of A have been observed in the Toledo formation (Figs. 2-9B to 2–9D). Channel fills in the Toledo formation are composed of predominantly of conglomerates and medium-grained sandstones (facies A and B) and exhibit fining upward trends. These channel fills range in thicknesses from approximately 0.5 to 7 m. Type B2 is generally observed as isolated channels indicating low sinuosity of the channel (Mutti and Normark, 1987, 1991). It is not possible to determine true channel width at outcrop scale.

Lobes

Lobes are characterized by absence of basal channeling, thickening upwards cycles, a range of sandstone grain size, laterally continuous beds, sheet-like geometry, and being largely enclosed in thin interbeds of sandstones and mudstones (especially in the lower fan setting; Shanmugan and Moiola, 1988). These deposits are laterally extensive with thicknesses of up to 10 m in outcrop of the Toledo formation (Figs.2-10A and 2-10B).

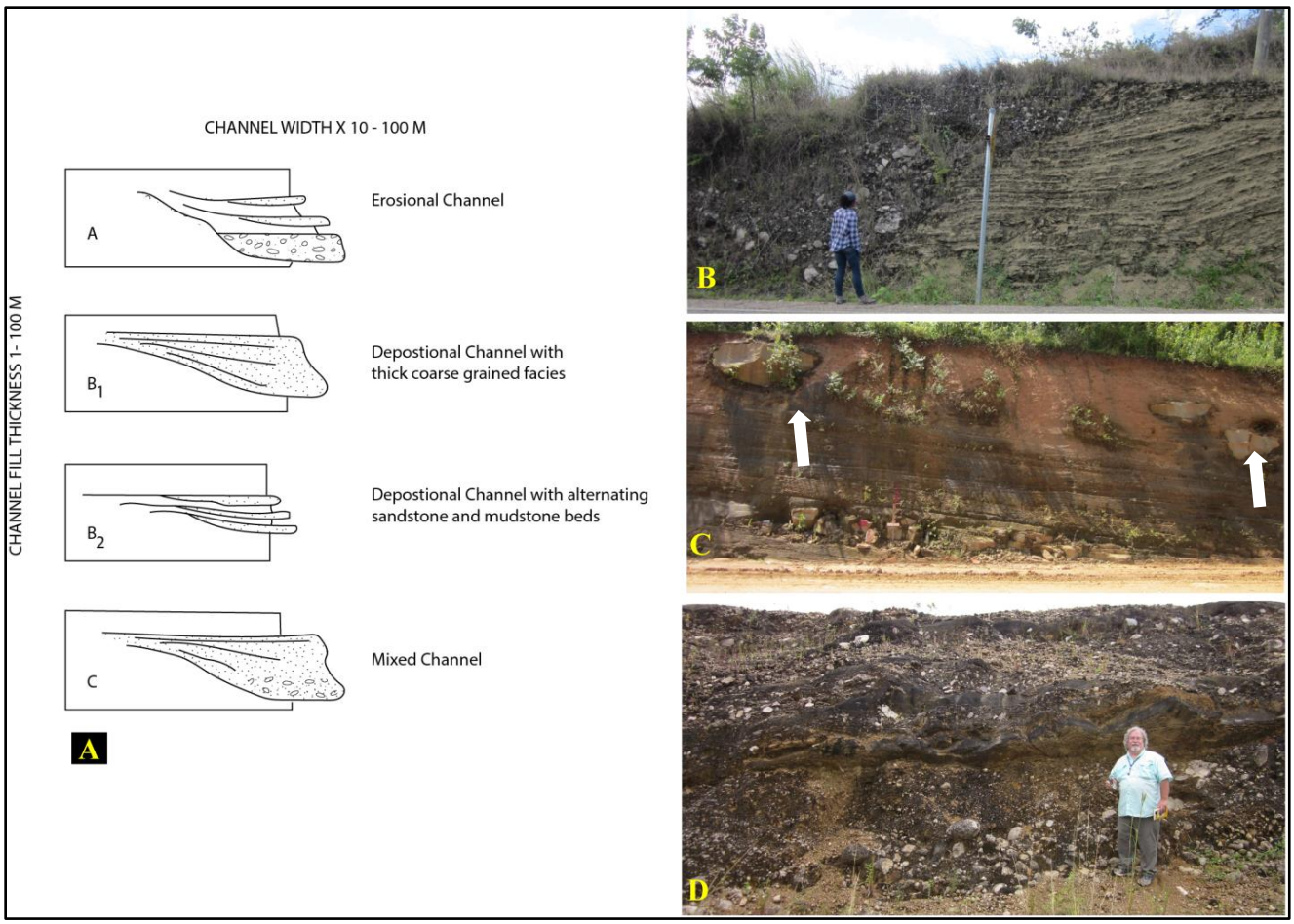

Figure 2-9: Examples of channel fills. (A) Channel fill (classified after Mutti and Normark, 1987, 1991, as noted in text); (B) thick coarse grained (conglomerate) depositional channel; (C) depositional channel in facies E showing smaller channels indicated by the arrows; and (D) mixed channel of conglomerate to sandstone.

Figure 2-10: Example of lobes. (A & B) Two examples of thin-bedded sandstone-mudstone interpreted as lobe deposits showing significant lateral continuity.

Sheet sands

Sheet sands are interbedded thin sandstones and mudstones and generally do not exhibit upward thickening trends. Lobes can be comprised of sheet sands, but not all sheet sands represent lobes. Sheet sands can also develop in broad channels in fan fringe areas, and associated with the lower fan (Shanmugan and Moiola, 1988). These are laterally extensive in the Toledo formation and reach thicknesses of up to 10 m.

Submarine Fan Facies Associations

Submarine fan facies associations are typically divided into outer fan, middle fan, submarine canyon, and shelf-derived deposits (Scholle and Spearing, 1982). Toledo facies associations are briefly described below.

Outer fan

The outer fan facies association is characterized by regularly interbedded mudstone and sandstone (couplets of facies C and D, as described earlier), which commonly exhibit thickening upwards cycles due to the progradational origin of depositional lobes. The sandstones show little channelization and have great lateral continuity. Facies B locally occurs at the top of thickening upwards cycles (Figs. 2-10A and 2-10B). Slumped and contorted facies D can be observed locally throughout the sequence and can be related to tectonic activity, sea-level changes, or seismic or other slope failure. The carbonate breccia (facies F) represents a debris flow and can be placed within this setting due to a lack of channeling.

Middle fan

The middle fan association, herein referred to as mid-fan, is generally characterized by the predominance of lenticular bodies of thick, medium- to coarse-grained, channelized sandstone and conglomerate units (facies A, B, and C). These facies commonly occur in couplets including facies B/E, A/B, and B/C. Thinning upwards cycles are common and they are interpreted to represent episodic channel migration (Scholle and Spearing, 1982). These are accompanied by facies C and D and occurrences of facies E in inter-channel regions (Figs. 2-4B, 2-9A, and 2-9C). These interchannel facies may be transitional to the depositional lobes of the outer fan. Failure along the flanks of the channel may result in contorted masses of facies C and pebbly mudstones of facies F.

Submarine canyon

Submarine canyon locations are characterized by major channel fill complexes of conglomerate, pebbly sandstone, and pebbly mudstone (facies A and F). For example, in Figure 2-7A, facies D can be observed overlying these deposits. These deposits are commonly associated with mudstone beds of facies F, which indicates abandonment (Scholle and Spearing, 1982). Pelagic and hemipelagic mudstones of facies G do not occur in the submarine canyon deposits.

Shelf-derived deposits

These deposits are characterized by thin beds of facies G limestones and are commonly interbedded with facies D (in particular facies D of the inter-channel/channel-lobe transition). These represent a reduction in clastic sedimentation (and or the erosion of an adjacent carbonate shelf) and likely represent either eustatic or local relative sea-level changes. These may also represent the transition between deeper water basin and shallow-water platform.

Summary

Owing to the well exposed stratigraphic sections in southern Belize, we were able to carry out lithofacies analysis on the deepwater clastics of the Toledo formation. We identified seven major lithofacies, facies A–G, and identified outcrop-scale architectural elements namely channel, lobe, and sheet sands. The existences of both channel and lobe deposits allow for the designation of submarine fan deposits to the

Toledo formation (Shanmugan and Moiola, 1988). Three major fan associations were identified: (1) outer fan/depositional lobe deposits, which are dominated by sheet like, laterally extensive non-channelized deposits of facies C/D, and local occurrences of facies F; (2) mid-fan deposits, which are characterized by channelized deposits of facies A–C with associated interchannel deposits of facies C–E and depositional channels having thick, coarse-grained facies, alternating sandstone and mudstone bed, and mixed channels; (3) submarine canyon deposits, consisting largely of facies A and F; and (4) shelf-derived deposits (facies G), characterized by thin-bedded carbonate units of wackestone-packstone deposited during episodes of adjacent shelfal erosion or subdued clastic sedimentation.

Acknowledgments

This research was supported in part by funding from the Big Creek Group, Independence, Belize. We are most grateful for their interest in and support of research on Belize geological history. In addition, J. F. thanks Ashley R. Jones for accompanying him into the field area. D. K.'s research was also supported by an Auburn University internal grant for research from the office of the Vice President for Research and Economic Development.

References

Fisher, J. D., and King, Jr., D. T., 2015, Stratigraphy of the Toledo formation, Belize basin, southern Belize: Gulf Coast Association of Geological Societies Transactions, v. 65, p. 107–123.

Fisher, J. D., King, D. T., Jr., and Da Gama, R. O. B. P., 2016, Submarine fan complex facies of the Paleogene Toledo formation in southern Belize: Boulder, Geological Society of America Abstracts with Programs, v. 48, no. 3, Abstract 28–1.

Lowe, D. R., 1982, Sediment gravity flows: II. Depositional models with special reference to the deposits of high density turbidity currents: Journal of Sedimentary Petrology, v. 52, p. 279–297.

Mulder, T., and J. Alexander, 2001, The physical character of subaqueous sedimentary density flows and their deposits: Sedimentology, v. 48, p. 269–299.

Mutti, E., and Ricci Lucchi, F., 1972, Le torbiditi dell|Apennino Settentrionale Introduzione all|analisi di facies: Memorie. Soc. Geoligica Italiana 11, p.161-199

Mutti, E., and Ricci Lucchi, F., 1975, Turbidite facies and facies associations. *In* Mutti E. et al. (eds.), Turbidite facies and facies associations in some selected formations of northern Apennines: IAS International Congress "Nice '75", Exc.Guidebook A-11, p. 21-36.

Mutti, E., and Normark, W.R., 1987, Comparing examples of modern and ancient turbidite systems: problems and concepts. *In* J.K. Leggett, G.G. Zuffa (Eds.), Marine Clastic Sedimentology concepts and case studies, Graham and Trotman, London (1987), p. 1–38

Mutti, E., and Normark, W.R., 1991, An integrated approach to the study of turbidite systems. *In* P. Weimer, M.H. Link (eds.), Seismic facies and sedimentary processes of submarine fans and turbidite systems, Springer, New York, p. 75–106.

NACSN (North American Commission on Stratigraphic Nomenclature), 2005, North American Stratigraphic Code: American Association of Petroleum Geologists Bulletin, v. 89, p. 1547–1591.

Purdy, E.G., Gischler, E., and Lomando, A.J., 2003, The Belize margin revisited, 2-Origin of Holocene antecedent topography: International Journal of Earth Sciences v. 92, No. 4, p. 552-572

Reading, H.G., and Richards, M., 1994, Turbidite systems in deep-water basin margins classified by grain size and feeder system: American Association of Petroleum Geologists Bulletin, v. 78, p. 792-822.

Ricci Lucchi, F., 1975a, Depositional cycles in two turbidite formations of northern Apennines: Journal of Sedimentary Petrology, v. 45, p. 1-43.

Ricci Lucchi, F., 1975b, Miocene paleogeography and basin analysis in the Periadriatic Apennines, *In* H.S. Coy (ed.), Geology of Italy, Earth Science Society of Libyan Arab Republic, Tripoli, p. 5-111.

Salvador, A., ed., 1994, International Stratigraphic Guide, 2nd ed.: Geological Society of America, Boulder, Colorado, 214 p.

Scholle, P.A., and Spearing, D., 1982, Sandstone depositional environments: American Association of Petroleum Geologists, 410 p.

Shanmugam, G., 2000, 50 years of the turbidite paradigm (1950s–1990s): deep-water processes and facies models—a critical perspective: Marine and Petroleum Geology, v. 17, p. 285-342.

Shanmugan, G., and Moiola, R.J., 1988, Submarine Fans: Characteristics, Models, Classification and Reservoir potential; Earth Science Review, v 24, p. 383 -428

Sprague, A. R., Sullivan M. D., Campion K. M., Jensen, G. N., Goulding, F. J., Garfield T. R., Sickafoose, D. K., Rossen, C., Jennette, D. C., Beaubouef , R. T., Abreu V., Ardill, J., Porter, M. L., and Zelt, F. B., 2002a, The physical stratigraphy of deep- water strata: A hierarchical approach to the analysis of genetically related elements for improved reservoir prediction, (Abstract): American Association of Petroleum Geologists Search and Discovery Article 90007, Tulsa, Oklahoma, <http://www.searchanddiscovery.com/abstracts/pdf/2002/annual/SHORT/ndx_41753.pdf> Last accessed August 4, 2014.

Sprague, A. R., Patterson, P. E., Hill, R.E., Jones, C.R., Campion, K. M., Van Wagoner, J.C., Sullivan, M. D., Larue, D.K., Feldman, H.R., Demko, T.M., Wellner, R.W., Geslin, J.K., 2002b, The physical stratigraphy of fluvial strata: A hierarchical approach to the analysis of genetically related stratigraphic elements for improved reservoir prediction, (Abstract): American Association of Petroleum Geologists Search and Discovery Article 90007, Tulsa, Oklahoma, <http://www.searchanddiscovery.com/abstracts/pdf/2002/annual/SHORT/ndx_41780.pdf> Last accessed August 4, 2014.

Stow, D.A.V., 1985, Deep-sea clastics: where are we and where are we going? *In* Brenchley, P.J. & Williams, B.P.J. (eds) Sedimentology: Recent Developments and Applied Aspects, Special Publication Geological Society of London, v. 18, p. 67–93.

Stow, D.A.V, and Mayall, M., 2000, Deep-water sedimentary systems: New models for the 21st century: Marine and Petroleum Geology, v. 17, p. 125-135. PII: S0264-8172(99)00064-1.

Vinson, G., 1962. Upper Cretaceous and Tertiary Stratigraphy of Guatemala: Bulletin of American Association of Petroleum Geologists v. 62, No. 4, p. 425 – 456.

Walker, R.G., and Mutti, E., 1973, Turbidite facies and facies associations, *In* Turbidites and Deep-water sedimentation: Pacific Section, Society of Economic Paleontology and Mineralogy, p. 119-157. .

3. PETROFACIES ANALYSIS OF THE TOLEDO FORMATION: IMPLICATIONS FOR CARBONATE DEPOSITION AND TECTONIC PROVENANCE

Jason D. Fisher and David T. King Jr.

Target Journal - *Journal of South American Earth Sciences*

Abstract

The Toledo formation in the Belize Basin of southern Belize is an informal Paleogene unit consisting of interbedded sandstone-mudstone, sandstones, conglomerates, and limestones exposed in southern Belize. The study was undertaken to determine the syndepositional environment of carbonates and provenance and tectonic setting of the sandstones. Petrofacies analysis of the carbonates reveal that skeletal grains are generally abundant and consist of an open-marine assemblage of crinoids and echinoids and a restricted marine assemblage of gastropods, foraminifera, and algae. Non-skeletal grains are generally rare to common and consist of oöids, peloids, and terrigenous grains. These strata are interpreted as slope deposits based on models described by Schlager. Analysis of the sandstones revealed an average composition of 34% quartz, 2% feldspar, and 64% lithic fragments; thus all samples are classified as lithic arenites. These lithic fragments include limestone (reworked) and a variety of igneous rocks. Diagenetic features of both carbonates and sandstones include cementation and reduction of existing pore spaces, silicification, and compaction. Ternary plots of framework mineralogy indicate derivation from a recycled

orogen possibly related to the collision of the North America and Caribbean tectonic plates, the Maya Mountains, and the Yucatán Platform.

Introduction

The informal Paleogene Toledo formation was studied in southern Belize, Central America. The formation is ~ 3000 m thick and occurs within the Belize basin which experienced a shift in sedimentation from largely carbonate-dominated to clastic dominated at the end of Cretaceous. The formation is composed of extensive sandstones interbedded with shales, siltstones, conglomerates, and carbonates. Sandstones are the dominant lithology found throughout the various facies of the formation. These sandstones have been described as poorly sorted calcarenites containing igneous rock fragments, limestone grains, and chert particles (Vinson, 1962). Carbonates are relatively minor constituents of the Toledo formation and occur as two major facies, carbonate breccia, and wackestone-packstone (Fisher and King 2016).

This study presents the results of textural and mineralogical analysis from samples collected during the 2016 field session. The main objectives of this study are: (1) identify the syndepositional environment of limestones within the Toledo formation; (2) petrographic characterization of sandstones; (3) assess the economic potential of the sandstones based on petrographic data; and (4) determine the provenance and tectonic setting of the sandstones.

Materials and Methods

Exposures of the Toledo formation along the Southern Highway and Mile 14 Highway to Dump, in southern Belize, were examined and sampled. Representative sandstone and carbonate samples were taken at 34 and 4 localities, respectively. Conventional optical study was made of 38 thin sections coupled with point counts carried out digitally, using JMicorVision. The JMicroVision software was developed for the visualization and analysis of petrographic images. Tools within the software allow for granulometric analysis and computerized point counting. This provides an alternative to conventional estimates of modal composition and is carried out on thin section photomicrographs. 4-6 photomicrographs were taken for each thin section with a count of 300 points for each thin section. Thirteen classes were defined for sandstones and 14 were identified carbonates (Tables 3-2 and 3-3). The default uniform random grid was utilized. The results of point counting are presented herein as volume percentage unless otherwise stated.

For the carbonates, we used the following terms for relative frequencies of allochemical grains (allochems) identified in the samples, very rare <2%, rare 2-5%, sparse 5-10%, common 10-30%, very common 30-50%, and abundant > 50%.These frequencies represent the percentage of total grains unless otherwise stated. The allochems are divided into skeletal and non-skeletal grains.

For sandstones, the framework detrital composition was based on methods of Dickinson (1985) and was plotted on ternary diagrams of Dickinson and Suczek (1979),

which feature three plate tectonic provenances. Details on this can be found in the provenance section herein.

Plate tectonics plays an important role in determining the characteristics of detrital grains of sandstones (Dickinson and Suczek, 1979; Dickinson et al, 1983; Bhatia, 1983; Roster and Korsch, 1986). The ratio of framework grains (quartz, feldspar, and lithic fragments) provides important evidence of the lithology of the source rocks. The method used follows the Dickinson (1985) scheme, briefly described below.

Dickinson (1985) described sandstones based on their detrital framework grain composition which is largely controlled by the tectonic setting of their provenance. The major provenance types related to continental sources identified are stable cratons, basement uplifts, magmatic arcs, and recycled orogens. Detailed descriptions of these provenance types can be found in Dickinson and Suczek (1979) and Dickinson (1985).

Based on Dickinson (1985), grain types are classified as monocrystalline quartz (Qm), polycrystalline quartz (Qp), total feldspar (F), volcanic/metavolcanic lithic fragments (Lv), and sedimentary/metasedimentary lithic fragments (Ls) (Table 3-1). Detrital modes are recalculated to 100% as the sum of the above mentioned grain types (Table 3-3). Carbonate grains (Lc) are not recalculated with other lithic fragments (Lv and Ls) due to the geochemical response during weathering and diagenesis, coupled with the potential for confusion of extra- (i.e., reworked) and intra- basinal carbonate grains (intraclasts, bioclasts, oöliths, peloids).

Table 3-1: Grain-type classification based on Dickinson (1985).

A. Quartzose Grains (Q = Qm + Qp)
   - Q = Total quartzose grains
   - Qm = monocrystalline quartz
   - Qp = polycrystalline quartz

B. Feldspar grains (F)

C. Unstable lithic fragments (L = Lv + Ls)
   - L = total unstable lithic fragments
   - Lv = volcanic/metavolanic lithic fragments

D. Total Lithic fragments (Lt = L + Qp)
   - Lc = extrabasinal detrital limestone (not included in L or Lt)

Table 3-2: Summary of point counting results (percentage) for carbonate samples from the Toledo formation. ** Classes are recalculated as a total percentage not including matrix and cement.

Sample	FTD14A	FTD28A	FTD41A	WP438
Point count classes (%)				
*Skeletal grains**				
Bioclasts	0.80	3.17	1.67	3.00
Mollusks	0.00	0.67	3.17	1.00
Echinoids	0.00	0.33	0.00	0.00
Foraminifera (planktic)	0.20	0.00	0.00	0.00
Foraminifera (unidentified)	0.20	0.17	0.67	0.33
Red Algae	0.40	11.50	6.33	8.00
*Non Skeletal grains**				
Oöid	8.40	0.00	0.00	0.00
Peloid	0.00	17.67	5.00	5.00
Quartz	3.90	0.00	0.00	1.33
Feldspar	0.30	0.00	0.00	0.00
Lithics	51.20	23.33	53.83	52.67
Matrix	1.40	3.17	0.50	0.00
Cement	33.20	40.00	28.83	28.67
*Skeletal grains***				
Bioclasts	1.22	4.84	2.55	4.59
Mollusks	0.00	1.02	4.84	1.53
Echinoids	0.00	0.51	0.00	0.00
Foraminifera (planktic)	0.31	0.00	0.00	0.00
Foraminifera (unidentified)	0.31	0.25	1.02	0.51
Red Algae	0.61	17.58	9.68	12.23
	2.45	24.21	18.09	18.86
*Non Skeletal grains***				
Oöid	12.84	0.00	0.00	0.00
Peloid	0.00	27.01	7.65	7.65
Quartz	5.96	0.00	0.00	2.04
Feldspar	0.46	0.00	0.00	0.00
Lithics	78.28	35.68	82.32	80.53

Carbonate Petrography

Skeletal grains

Skeletal grains account 2 to 24% of the samples and consist of fragments of invertebrate and algal body fossils (Table 3-2). Some skeletal grains are classified as bioclasts due to loss of distinguishing features by diagenesis. Based on the skeletal grains identified we can interpret two assemblages, an open- and restricted-marine assemblages. The open-marine assemblage is very rare (about 1% of all skeletal grains) and consists of echinoids and corals (Figs. 3-1 and 3-2).Organisms within this assemblage is thought to require normal marine conditions for life.

A restricted marine assemblage is known to be tolerant of adverse environmental conditions namely variations in salinity. This assemblage is very rare to common (1 to 19% of skeletal grains) and consists of red algae, gastropods (mollusks), and foraminifera, in order of decreasing abundance (Figs. 3-1 and 3-2).

The skeletal grains generally lack evidence of transport and abrasion, i.e., little or no rounding. This suggests that initial deposition may have taken place in relatively low energy environments.

Non-skeletal grains

Non-skeletal grains make up between 62 to 97% of the samples and consist of carbonate lithic fragments, peloids, and terrigenous grains (Figs 3-1 and 3-2). Lithic fragments make up the majority of the non-skeletal grains within the samples ranging from 52 – 80%. Lithic fragments are dominated by reworked limestone which are

typically micritized clasts of varying sizes and possess skeletal grains of various sizes within. Igneous/metamorphic lithic fragments are generally rare to common throughout the samples. Quartz and feldspar grains are generally rare to sparse and may have originated from pre-existing (?) sandstones of the Toledo formation.

Peloids are grains typically composed of micrite, lacking internal structure. In some instances, it is difficult to distinguish reworked limestone clasts from peloids. In the samples, the peloids are generally sparse to common (Table 3-3).

Sandstone Petrography

Sandstones are the dominant lithology found throughout the various deep-water facies of the Toledo formation. These sandstones have been described as poorly sorted calcarenites containing igneous lithic fragmens, limestone grains, and chert (Vinson, 1962). Petrographic analysis in this study classified the Toledo sandstones as lithic arenites, differing from Vinson (1962) who classified them as calcarenites.

Texturally, the sandstones are poorly sorted, with angular to rounded grains. The sandstones are mainly grain supported with generally less than 15% matrix. Most intergranular pores are filled with cement. Based on this, they can be texturally classified as submature arenites (Boggs, 2006).

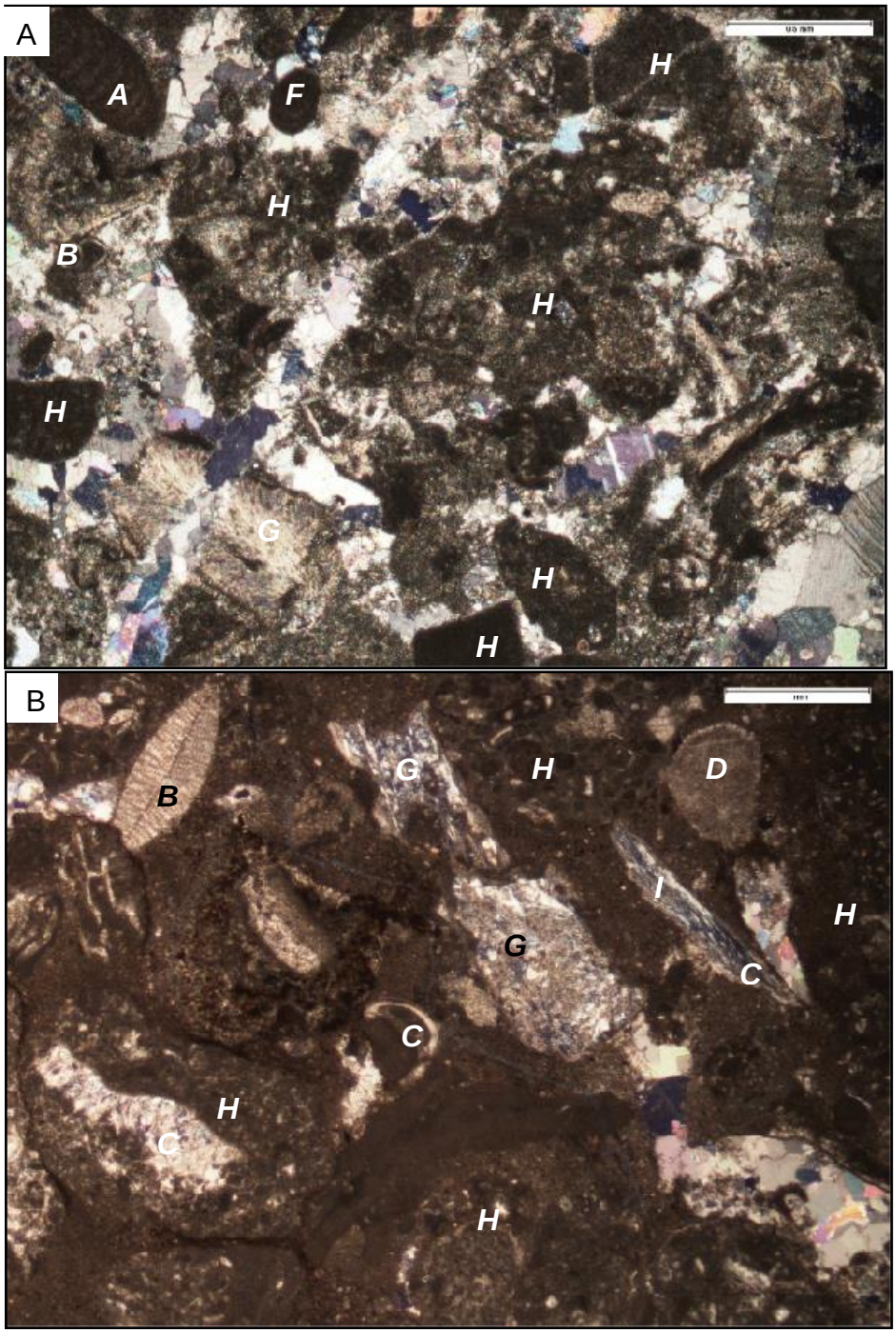

Figure 3-1: Photomicrographs of carbonate allochems and diagenetic features. Allochems: *A* - red algae, *B* - foraminifera, *C* - molluscs, *D* - echinoderms, *F* - peloid , *G* – bioclast, *H* - lithics, and *I* – quartz. Diagenetic features – coarse and fined grained calcite cement, silicification, and minor compaction. Scale for Fig. 3-1A and Fig 3-1B are 0.5 and 1 mm respectively.

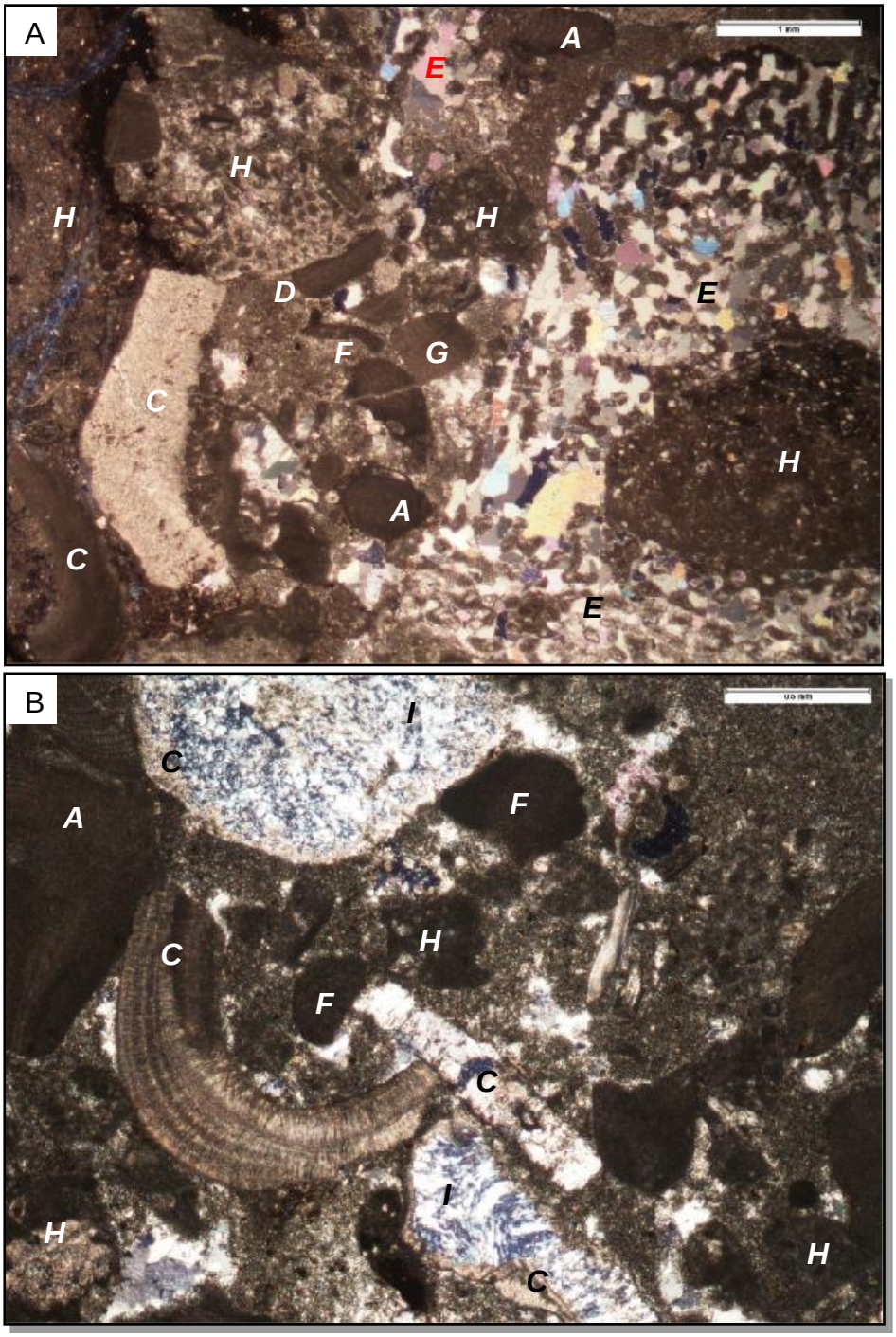

Figure 3-2: Photo-micrographs of carbonate allochems and diagenetic features. Allochems: *A* - red algae, *B* - foraminifera, *C* - mollusks, *D* - echinoderms, *E* - coral, *F* - peloid , *G* – bioclast, *H* - lithics, and *I* – quartz. Diagenetic features – coarse and fined grained calcite cement, silicification (represented by presence of chalcedony/chert), and minor compaction. Scale for Fig. 3-2A and Fig 3-2B is 0.5 and 1mm respectively.

Compositionally, the sandstones are dominated by lithic fragments, followed by quartz, with rare amounts of feldspars (by volume) (Table 3-3; Fig. 3-3). Thus, they can be classified as immature to submature lithic arenites. The lithic fragments are dominated by carbonate grains, particularly limestone and skeletal fragments, followed by igneous and unidentified lithics. The limestone grains are fossiliferous to un-fossiliferous and the grains are typically micritized, thus destroying most features within the grains. The fossil fragments include corals, algae, and foraminifera (benthic discocyclinids, unidentified benthics and planktics). Many fossils may have been weathered from larger micritic grains as suggested by their similar micritic coating in the micritized carbonate grains themselves. This inferred process suggests recycling of sediments from older sedimentary rock units. To some extent, all fossils have been affected by recrystallization and cementation.

A variety of igneous rock fragments have been observed (Fig. 3-3). Fine-grained clasts commonly possess laths of plagioclase and quartz in a fined-grained crystalline groundmass. Some do not possess phenocrysts making identification more difficult. Coarse-grained fragments commonly consist of polycrystalline quartz, mica, fine-grained fragments, and opaque minerals. There are also ultramafic and mafic lithic fragments that could potentially be serpentinite, peridotite, greenstones, or amphibolites.

Quartz grains include monocrystalline, polycrystalline, and sheared/stretched composite quartz (Fig. 3-3). The monocrystalline quartz commonly contains inclusions of plagioclase (?) and unidentifiable inclusions. Rare feldspar grains in the samples include plagioclase, orthoclase, and perthite (?). Rare occurrences of zoning in feldspar

are also observed. Accessory grains in the sandstones include mica and organic matter (Fig. 3-3).

A high percent of lithic fragments and textural features, such as poor to moderate sorting and angular to rounded grains, in the sandstones indicate transportation from nearby sources. The presence of angular feldspars is indicative of a high relief source area that experienced rapid erosion (Boggs, 2001).

Diagenesis

Diagenesis describes post depositional changes. In this study, porosity, cementation (porosity occlusion), and silicification were considered. Of the various types described in literature (Adams et al, 1997), three major types of porosity are identified in the Toledo samples: inter-, intra-particle (primary porosity), and fracture (secondary porosity) porosity. However, these pore spaces have been occluded by cement.

Three calcite cement generations are identified in the samples. The first is a rim of fine grained sparry crystals with a fibrous habit coating intra-particle pore spaces (Figs. 3-1, 3-2, 3-3, and 3-4). The second is a fine-grained sparry cement occluding intra- and inter- particle pore spaces and fracture pores (Figs. 3-1, 3-2, 3-3, and 3-4). The third is medium to coarse blocky/equant cement that also occludes intra- and interparticle pore spaces and fracture pores (Figs. 3-1, 3-2, 3-3, and 3-4). There is an overall increase in crystal size from the pore margins to the center (drusy mosaic). The patterns of cementation are consistent with marine phreatic (fibrous calcite cement) and meteoric phreatic zones (equant calcite cement and drusy mosaic) (Longman, 1980).

Table 3-3: Framework components obtained from point count data. All values are reported in percentage.

Sample Number	06A	07B	10	12A	13	16A	18A
Total quartz (% framework)	9.67	9.00	13.95	16.67	7.67	8.67	16.33
Total monocrystalline quartz (% framework)	8.00	5.33	10.30	12.67	5.67	7.33	12.00
Total polycrystalline quartz (% framework)	1.67	3.67	3.65	4.00	2.00	1.33	4.33
Total feldspar (% framework)	0.33	0.00	0.00	2.00	2.33	1.33	0.33
Total carbonate lithics (% framework)	22.67	13.67	0.00	1.33	10.00	8.00	13.00
Total Igneous grains (% framework)	29.00	35.00	29.24	28.00	24.67	30.00	13.67
Total unidentified Lithics (% framework)	12.67	15.67	22.92	22.33	24.33	16.00	6.33
Total fossil (% framework)	2.33	2.67	0.00	0.00	0.00	0.00	0.33
Total organic matter (% framework)	0.00	0.00	0.00	0.00	0.00	0.00	6.67
Total mica (% framework)	0.00	0.00	0.33	0.67	0.00	0.33	0.67
Total matrix(% framework)	2.00	2.67	10.96	17.67	17.67	13.67	13.00
Total cement (% framework)	21.33	21.33	22.59	11.33	12.33	22.00	29.67
Total pore (% framework)	0.00	0.00	0.00	0.00	1.00	0.00	0.00
Q - total quartz (Dickinson) (% total QFL)	29.00	20.46	32.31	35.71	22.12	21.67	53.85
F- feldspathic components (Dickinson) (% total QFL)	1.00	0.00	0.00	4.29	6.73	3.33	1.10
L -lithic components (Dickinson) (% total QFL)	87.00	79.55	67.69	60.00	71.15	75.00	45.05
Qm- monocrystalline quartz (Dickinson) (% total QmFL)	20.51	12.10	23.85	27.14	16.35	18.33	39.56
F- feldspathic components (Dickinson) (% total QmFL)	0.85	0.00	0.00	4.29	6.73	3.33	1.10
Lt -lithic components (Dickinson) (% total QmFL)	78.63	87.90	76.15	68.57	76.92	78.33	59.34

Table 3-3 continued

Sample Number	24A	32.2	34A	36A	42A	46A	50B
Total quartz (% framework)	8.33	21.67	7.33	5.33	16.00	11.67	21.67
Total monocrystalline quartz (% framework)	7.00	16.67	5.33	4.00	14.00	10.00	19.67
Total polycrystalline quartz (% framework)	1.33	5.00	2.00	1.33	2.00	1.67	2.00
Total Feldspar (% framework)	0.33	1.00	2.33	2.33	1.00	0.00	0.00
Total carbonate lithics (% framework)	26.67	10.00	26.33	30.00	18.33	27.00	25.00
Total Igneous grains (% framework)	19.00	21.67	19.33	26.00	16.33	23.33	24.33
Total unidentified Lithics (% framework)	8.33	15.00	3.00	3.67	1.67	0.00	0.67
Total fossil (% framework)	0.00	0.00	0.33	0.67	0.33	0.33	1.67
Total organic matter (% framework)	0.00	0.00	0.00	0.00	4.33	0.00	0.00
Total mica (% framework)	0.00	1.00	0.00	0.00	0.00	0.00	0.33
Total matrix(% framework)	6.67	7.67	5.67	0.00	11.00	0.33	3.67
Total cement (% framework)	30.67	22.00	35.67	31.00	31.00	37.33	22.67
Total pore (% framework)	0.00	0.00	0.00	1.00	0.00	0.00	0.00
Q - total quartz (Dickinson) (% total QFL)	30.12	48.87	25.29	15.84	50.94	33.33	47.10
F- feldspathic components (Dickinson) (% total QFL)	1.20	2.26	8.05	6.93	2.83	0.00	0.00
L -lithic components (Dickinson) (% total QFL)	68.67	48.87	66.67	77.23	46.23	66.67	52.90
Qm- monocrystalline quartz (Dickinson) (% total QmFL)	25.30	37.59	18.39	11.88	39.62	28.57	42.75
F- feldspathic components (Dickinson) (% total QmFL)	1.20	2.26	8.05	6.93	2.83	0.00	0.00
Lt -lithic components (Dickinson) (% total QmFL)	73.49	60.15	73.56	81.19	57.55	71.43	57.25

Table 3-3 continued

Sample Number	51A	58A	59A	62A	72A	74A	75A
Total quartz (% framework)	7.67	23.33	21.33	11.00	12.00	9.33	12.67
Total monocrystalline quartz (% framework)	6.33	17.67	16.00	9.33	10.00	7.67	8.33
Total polycrystalline quartz (% framework)	1.33	5.67	5.33	1.67	2.00	1.67	4.33
Total Feldspar (% framework)	0.33	0.33	0.33	0.33	0.67	1.00	0.33
Total carbonate lithics (% framework)	29.67	20.67	20.67	29.00	21.00	19.33	20.33
Total Igneous grains (% framework)	24.00	19.33	27.67	16.33	22.67	19.67	26.00
Total unidentified Lithics (% framework)	0.67	0.33	1.33	0.67	3.00	1.33	0.67
Total fossil (% framework)	2.67	2.00	4.67	5.33	0.33	1.00	0.33
Total organic matter (% framework)	0.00	0.00	0.00	0.00	0.33	0.00	0.00
Total mica (% framework)	0.00	0.00	0.00	0.00	0.00	0.33	0.00
Total matrix(% framework)	1.33	1.67	4.00	3.00	4.33	2.00	1.33
Total cement (% framework)	33.67	32.33	20.00	34.33	35.67	46.00	38.33
Total pore (% framework)	0.00	0.00	0.00	0.00	0.00	0.00	0.00
Q - total quartz (Dickinson) (% total QFL)	23.96	54.26	43.24	39.76	33.96	31.11	32.48
F- feldspathic components (Dickinson) (% total QFL)	1.04	0.78	0.68	1.20	1.89	3.33	0.85
L -lithic components (Dickinson) (% total QFL)	75.00	44.96	56.08	59.04	64.15	65.56	66.67
Qm- monocrystalline quartz (Dickinson) (% total QmFL)	19.79	41.09	32.43	33.73	28.30	25.56	21.37
F- feldspathic components (Dickinson) (% total QmFL)	1.04	0.78	0.68	1.20	1.89	3.33	0.85
Lt -lithic components (Dickinson) (% total QmFL)	79.17	58.14	66.89	65.06	69.81	71.11	77.78

Table 3-3 continued

Sample Number	76A	77c	78A	79D	79E	80A
Total quartz (% framework)	15.00	15.67	9.33	3.67	12.67	23.33
Total monocrystalline quartz (% framework)	13.33	13.33	7.00	2.67	10.33	17.67
Total polycrystalline quartz (% framework)	1.67	2.33	2.33	1.00	2.33	5.67
Total Feldspar (% framework)	1.00	0.33	0.00	0.00	0.67	1.33
Total carbonate lithics (% framework)	26.00	27.00	28.67	43.00	28.00	19.00
Total Igneous grains (% framework)	29.00	19.33	18.33	16.00	30.33	25.67
Total unidentified Lithics (% framework)	0.67	1.00	0.00	0.00	0.00	0.33
Total fossil (% framework)	0.00	0.67	1.67	4.00	1.67	0.00
Total organic matter (% framework)	0.00	0.00	0.67	0.00	0.00	1.67
Total mica (% framework)	0.33	0.67	0.00	0.00	0.00	1.00
Total matrix(% framework)	1.67	0.67	0.00	0.00	3.33	2.67
Total cement (% framework)	26.33	34.67	41.33	33.33	23.00	25.00
Total pore (% framework)	0.00	0.00	0.00	0.00	0.33	0.00
Q - total quartz (Dickinson) (% total QFL)	48.57	44.34	33.73	18.64	28.79	46.36
F- feldspathic components (Dickinson) (% total QFL)	1.71	0.94	0.00	0.00	1.52	2.65
L -lithic components (Dickinson) (% total QFL)	49.71	54.72	66.27	81.36	69.70	50.99
Qm- monocrystalline quartz (Dickinson) (% total QmFL)	22.86	37.74	25.30	13.56	23.48	35.10
F- feldspathic components (Dickinson) (% total QmFL)	1.71	0.94	0.00	0.00	1.52	2.65
Lt -lithic components (Dickinson) (% total QmFL)	75.43	61.32	74.70	86.44	75.00	62.25

Table 3-3 continued

Sample Number	WP395	WP396	WP398	WP401	WP405	WP427	WP428
Total quartz (% framework)	13.67	14.33	8.00	15.00	18.33	21.33	11.33
Total monocrystalline quartz (% framework)	11.33	11.67	4.67	12.33	15.33	17.33	9.33
Total polycrystalline quartz (% framework)	2.33	2.67	3.33	2.67	3.00	4.00	2.00
Total feldspar (% framework)	1.00	1.00	2.33	0.00	1.00	0.33	0.00
Total carbonate lithics (% framework)	16.00	28.67	19.67	26.67	7.00	23.33	43.00
Total Igneous grains (% framework)	37.67	23.00	40.00	23.67	49.00	25.67	25.00
Total unidentified Lithics (% framework)	2.00	3.00	1.67	2.67	4.00	2.67	2.00
Total fossil (% framework)	2.00	0.00	0.00	0.67	0.00	0.33	3.00
Total organic matter (% framework)	0.00	0.00	3.33	0.33	0.00	0.00	0.00
Total oica (% framework)	0.00	0.00	0.00	0.00	0.00	0.00	0.00
Total matrix(% framework)	0.33	3.33	0.67	0.00	1.00	3.33	0.67
Total cement (% framework)	27.33	26.67	24.33	31.00	19.67	23.00	15.00
Total pore (% framework)	0.00	0.00	0.00	0.00	0.00	0.00	0.00
Q - total quartz (Dickinson) (% total QFL)	26.11	37.39	15.89	38.79	26.83	45.07	31.19
F- feldspathic components (Dickinson) (% total QFL)	1.91	2.61	4.64	0.00	1.46	0.70	0.00
L -lithic components (Dickinson) (% total QFL)	71.97	60.00	79.47	61.21	71.71	54.23	68.81
Qm- monocrystalline quartz (Dickinson) (% total QmFL)	21.66	30.43	9.27	31.90	22.44	36.62	25.69
F- feldspathic components (Dickinson) (% total QmFL)	1.91	2.61	4.64	0.00	1.46	0.70	0.00
Lt -lithic components (Dickinson) (% total QmFL)	76.43	66.96	86.09	68.10	76.10	62.68	74.31

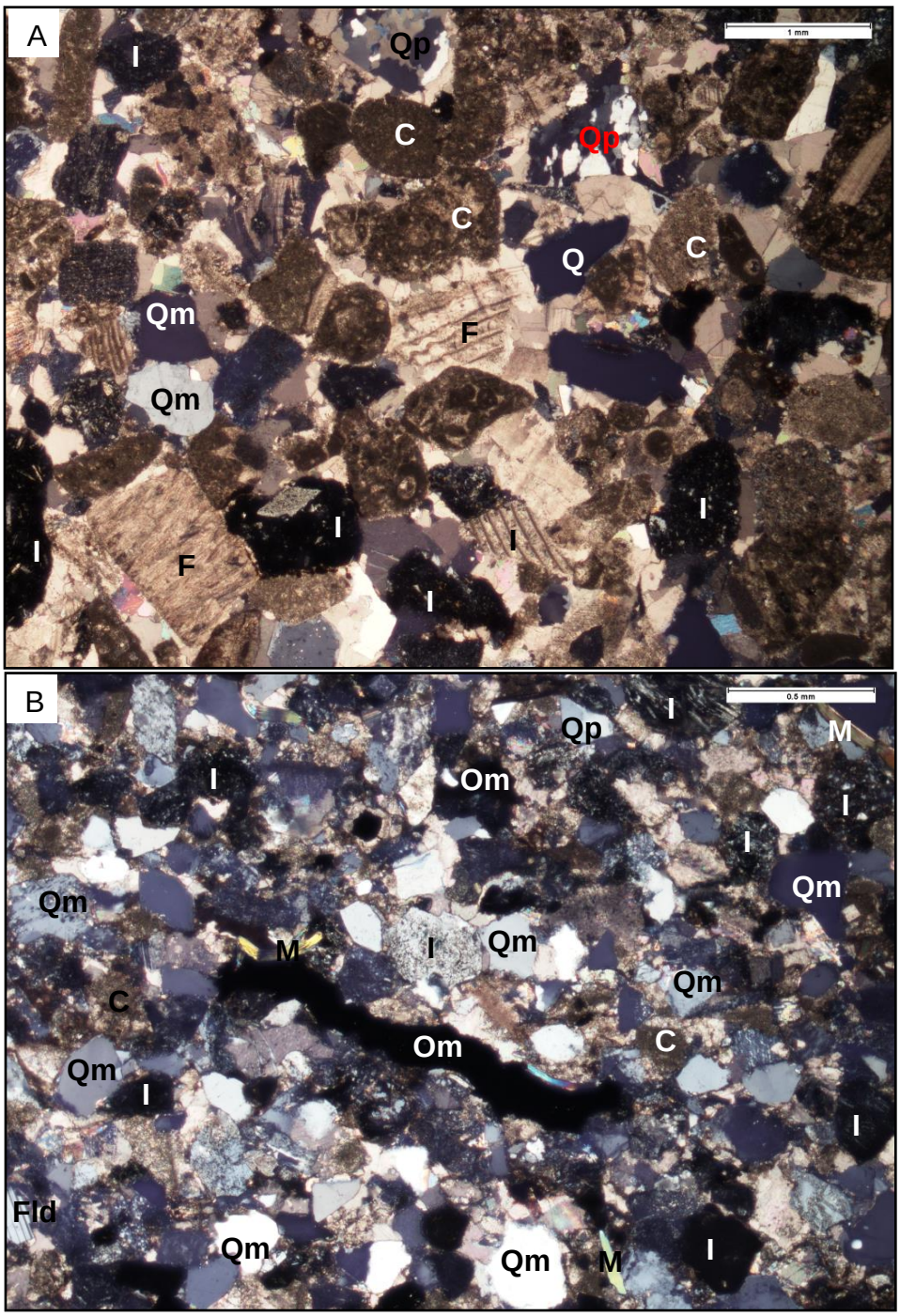

Figure 3-3: Photomicrographs of Toledo sandstones showing igneous grains (I), carbonate grains (reworked, micritized [C] and fossil fragments [F]), quartz (poly [Qp] and mono [Qm]), feldspar (Fld), organic matter (Om), and mica (M). Flexible deformation observed in mica grains (compaction). Scale for Fig. 3-3A and Fig 3-3B are 1 and 0.5 mm respectively.

Secondary quartz as overgrowths on detrital grains (monocrystalline quartz) is rare (Fig. 3-5). These overgrowths may represent pre-existing silica cement from sediment source.

Silicification is relatively rare throughout the samples and occurs as an inter-particle pore filling variety of microquartz, possibly chert (Figs. 3-1, 3-2, 3-3, and 3-4). This selectively occurs in skeletal grains, destroying its original fabric, making identification difficult.

The effect of physical compaction is minor and is largely observed as micro-fractures, flexible grain deformation, and concavo-convex and long contacts. Micro-fractures in the samples appear to only affect particular grains, including carbonate and igneous grains and micas largely represented in the sandstone samples (Figs. 3-1, 3-2, 3-3, and 3-4). Micas exhibit flexible grain deformation (Fig. 3-3). Concavo-convex and long contacts are seen between lithic fragments (igneous and sedimentary), quartz, and feldspar grains (Fig. 3-5 and 3-6).

Economic Potential

Reservoir development is largely dependent on the original sandstone composition, which in turn influenced by sediment source and tectonic history. The Toledo sandstones are texturally submature and mineralogically immature. Texturally immature sandstones typically display less porosity and permeability, thus decreasing the reservoir potential. Reservoir quality is also affected by subsequent diagenesis of the sandstones. Porosity occlusion points to the poor reservoir rock potential of the sandstones whether for oil and gas or groundwater resources. However, the porosity

occlusion coupled with thick interbeds of mudstone and siltstone and the formation's extensive thickness, suggests that the Toledo may serve as a good seal potential for the Cretaceous reservoirs. The sandstones also display stratigraphic trapping potential as a diagenetic barrier due to porosity occlusion.

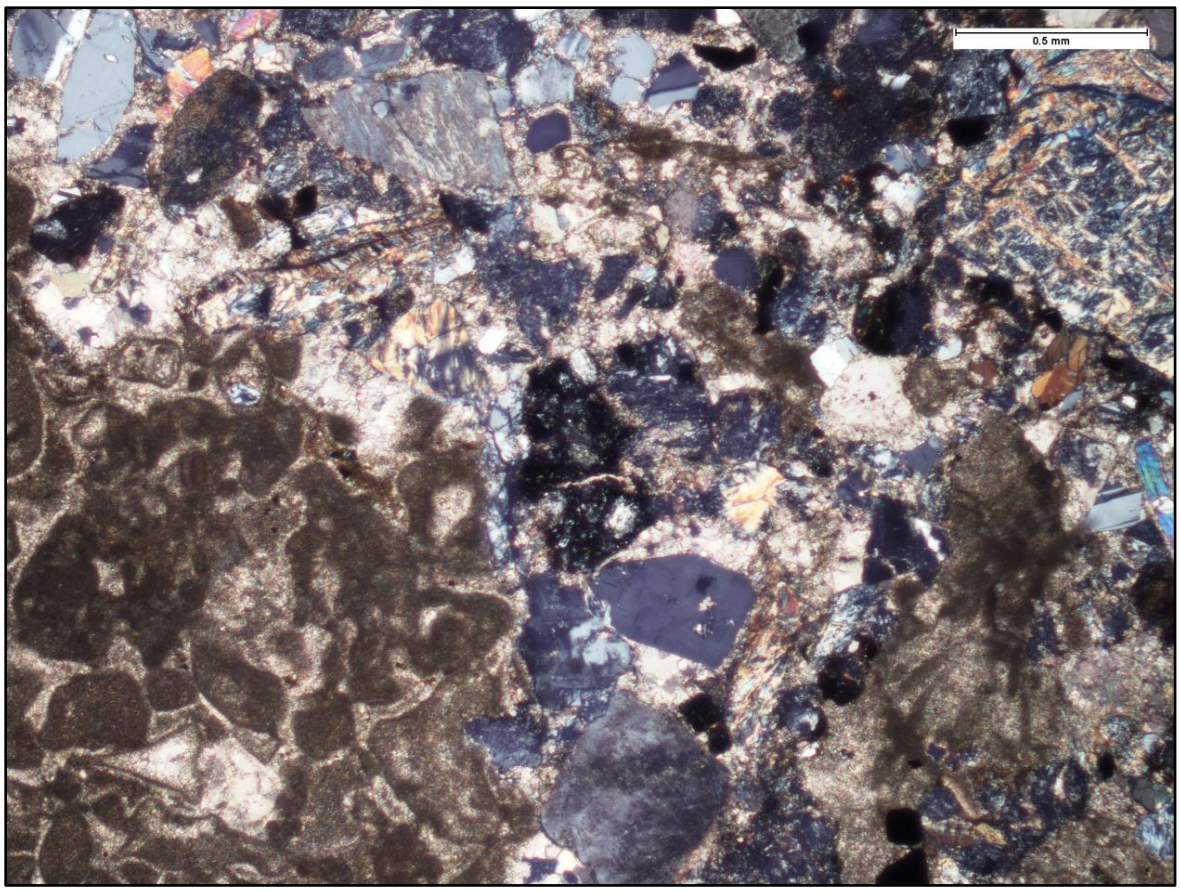

Figure 3-4: Photomicrograph of Toledo sandstones showing diagenetic features: fine and coarse grained calcite cement, minor silicification in carbonate grain in the bottom left, fracture in lithic and quartz grains (compaction), and concavo-convex and long contacts are seen between lithic fragments. Scale for Fig. 4-5A is 0.5 mm.

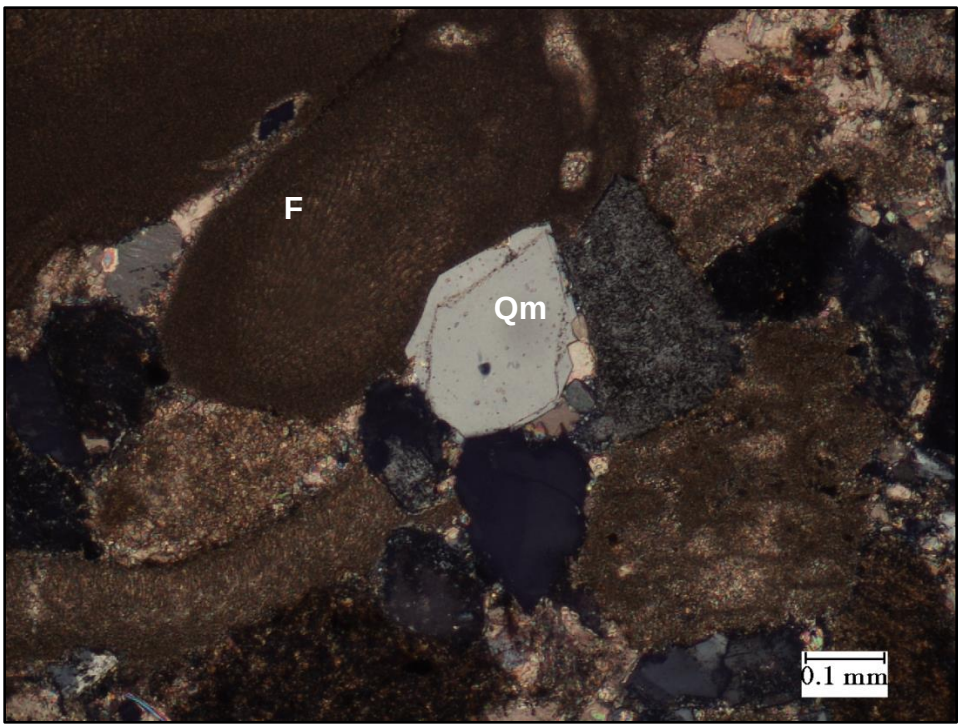

Figure 3-5: Photomicrograph of Toledo sandstone showing diagenetic features: quartz overgrowth, and long contact between quartz grain (Qm) and fossil fragment (F). Scale is 0.1 mm

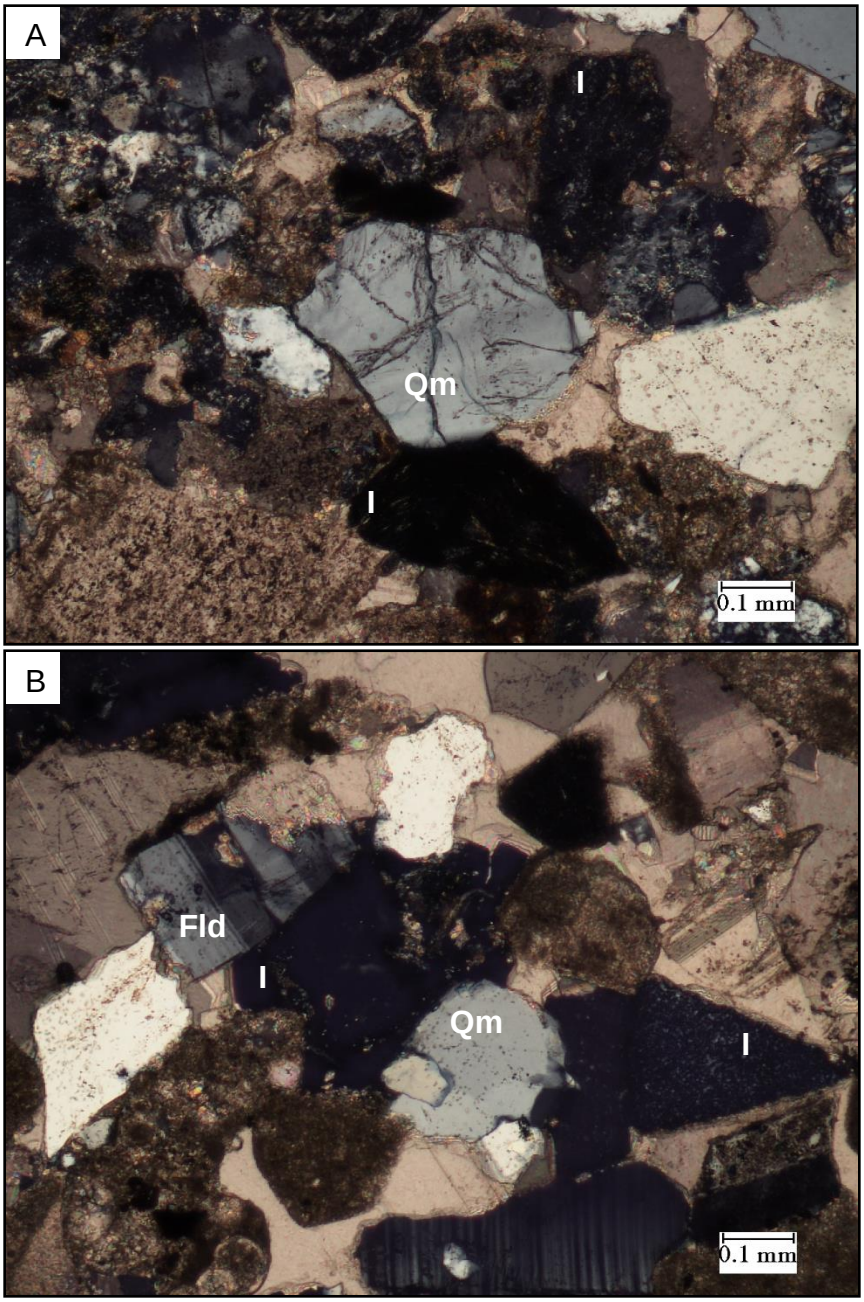

Figure 3-6: Photomicrographs of Toledo sandstones showing diagenetic features. (A) Physical compaction between quartz and igneous lithic fragment as concavo-convex contacts. (B) Physical compaction between feldspar (Fld), igneous lithic fragment (I), and quartz grain (Qm). Scale is 0.1 mm.

Carbonate Depositional Setting

Based on the locality of the study area and the facies described, the depositional environment for the Toledo carbonates is within the T Carbonate factory (per Schlager, 2005). The 'T' represents tropical or 'top of the water column' and is limited to the tropical zone between 30°N and 30°S. Schlager (2005) described several facies within this carbonate factory. Our samples potentially matches two of Schlager's facies, namely facies 2 (deep shelf) and facies 4 (slope) (Fig. 3-7).

Facies 2 is described as typically being located below fair-weather wave base, but within reach of storm waves in close proximity to the euphotic zone. Deep shelves also form plateaus between active platform and deeper basin (established on top of drowned platforms). The facies is characterized by skeletal wackestone and some grainstone, bioturbation, and the presence of shelly fauna indicating normal marine conditions.

Facies 4, deposited on a slope, is typically located seaward of a platform margin and consists of predominantly of re-worked platform admixtures with highly variable grain sizes. This facies consists of mostly re-deposited shallow-water benthics and some deep water benthics and plankton.

The carbonate samples from the Toledo formation are dominated by reworked lithic grains of various sizes. The skeletal grains are dominated by shallow-water benthics particularly algae, mollusks, and foraminifera (both benthic and planktic). This suggests that the facies 4 – slope model is the best fit for these limestones.

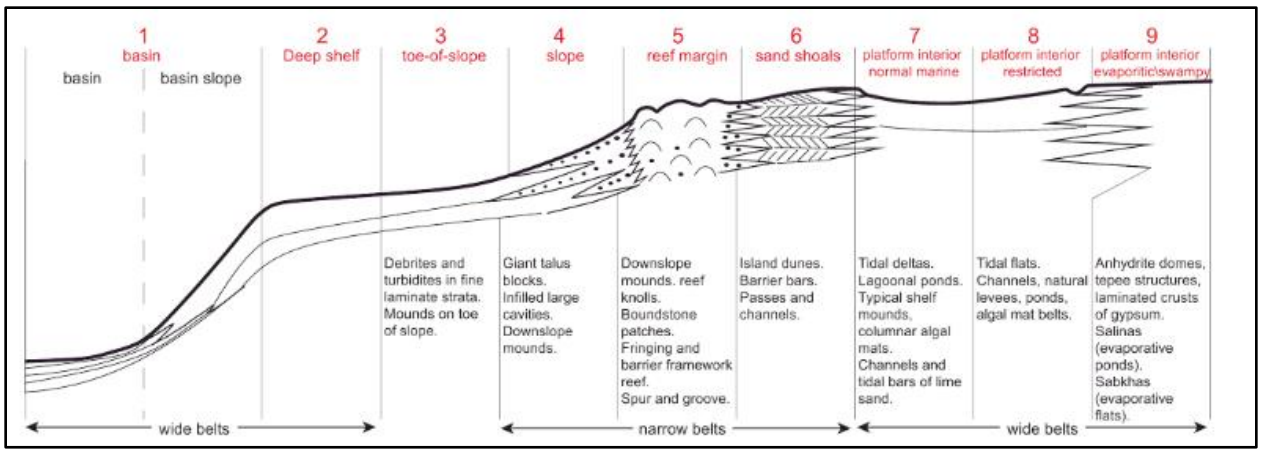

Figure 3-7: Outline of standard facies with name and number of facies labeled in red. The cross section shows sediment geometry and list fine scale features for each facies. Modified after Schlager (2005).

Provenance

Two ternary diagrams of Dickinson (1985) were used for this study: QFL and QmFLt ternary plots. The QFL diagram emphasizes grain stability and maturity and hence focuses on weathering, provenance relief, transport, and source rock based on total quartz, feldspar and lithics (Dickinson and Suczek, 1979; Dickinson, 1985). On this ternary diagram, our data largely plots as recycled orogen with some samples falling in the magmatic arc (undissected and transitional arc) provenance fields (Fig. 3-8). The emphasis of QmFLt ternary diagram is on source rock where all unstable lithic fragments (Qp, Lv, and Ls) are plotted together as Lt (see Table 3-3). All our sample data plotted within the recycled orogen field between transitional and lithic orogen (Fig. 3-9). Orogenic recycling occurs in several tectonic settings where rocks are deformed, uplifted and eroded. There settings include subduction complexes, backarc thrust belts, and suture belts.

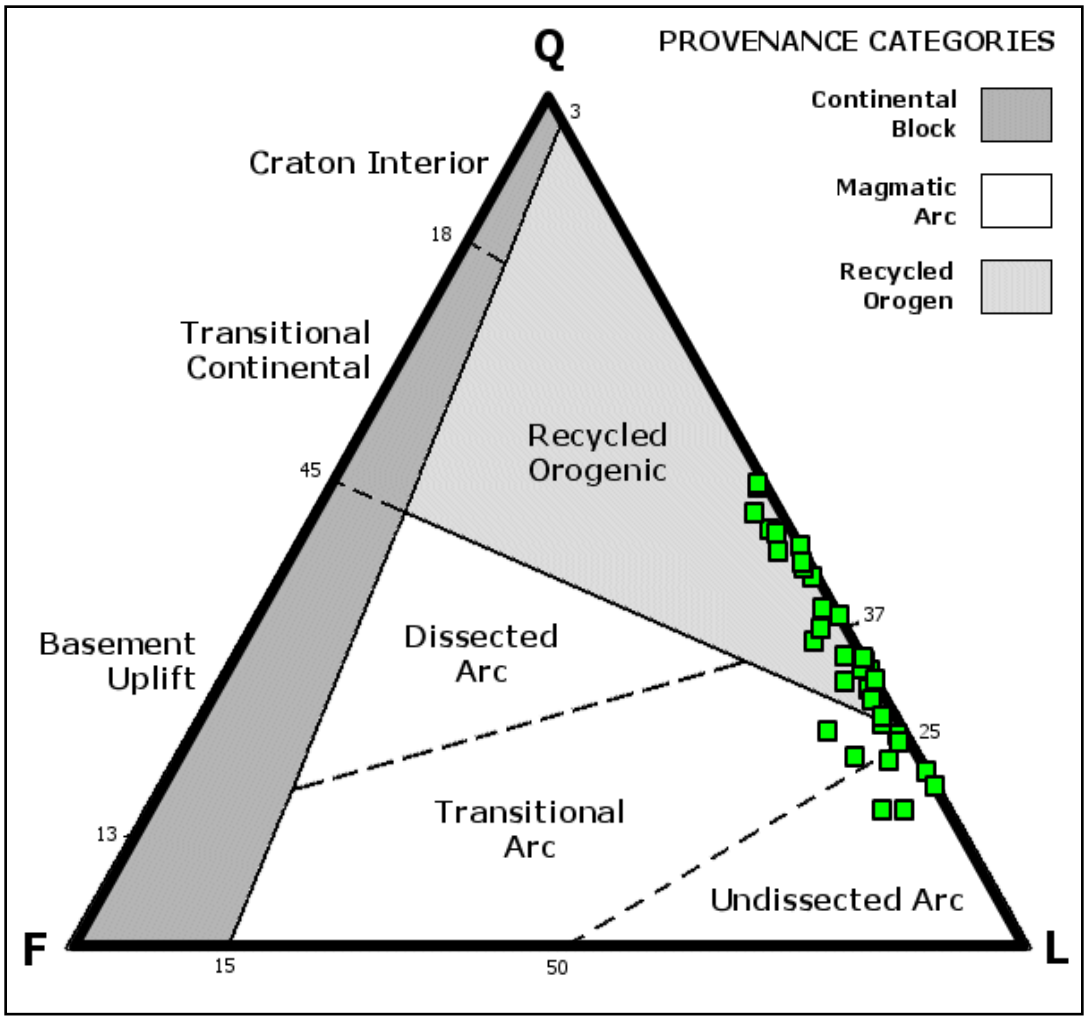

Figure 3-8: QFL plot of the Toledo formation sandstones according to Dickinson (1985).

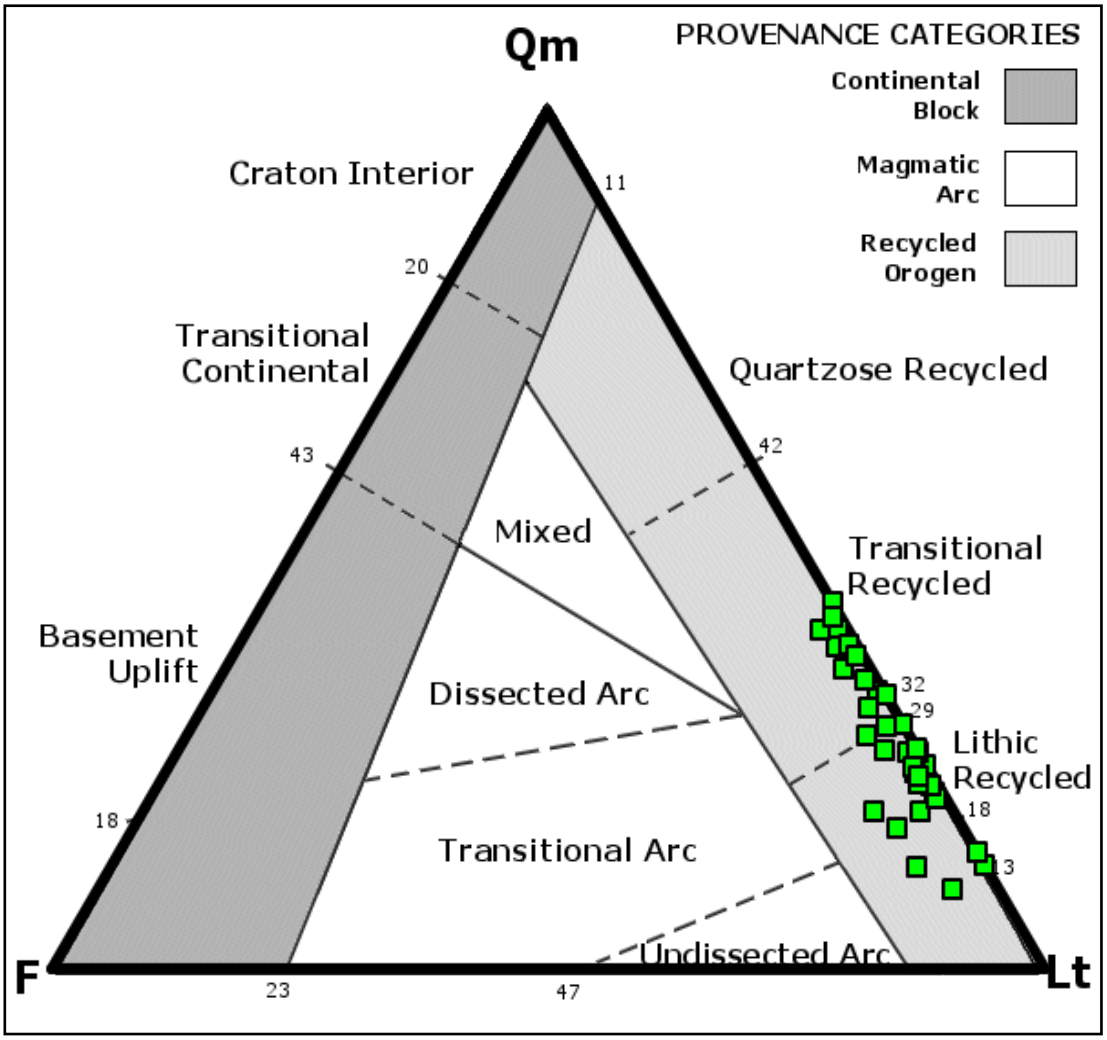

Figure 3-9: QmFLt plot of the Toledo formation sandstones according to Dickinson (1985).

The Belize basin is the eastern extension of the Chapayal basin in Guatemala, located south of the La Libertad Arch and Maya Mountains (Vinson, 1962). The basin also sits on the northern edge of the folded and faulted mountains (mainly limestone) and a metamorphic and volcanic complex referred to as a geanticline (anticline of

regional extent) by Vinson (1962). The collision of the North American and Caribbean plates created the Motagua-Polochic fault system, which passes just south of Belize near the southern limit of the Belize Basin (Ramanathan and Garcia, 1991; Leroy et al., 2000). During this time, an accretionary complex was developed by the fault system onshore Guatemala known as the El Tambor complex, more recently referred to as the Motagua suture complex, just south of the Belize basin (Case, 1980; Fig. 4.8). The complex includes a suite of ultramafic to mafic rocks (including serpentinite, serpentinite melange, peridotite, mylonized gabbro and diorites, greenstones, and amphibolites), low grade metamorphic sediments, and metamorphosed pillow lavas and chert (Case, 1980). The El Tambor complex (Fig. 3-10) is the suggested source of the ultramafic and mafic grains present in the Toledo sandstones.

Quartz grains show a clear dominance of monocrystalline over polycrystalline quartz, suggesting sediments were derived from a granitic source. The Maya Mountains and the Motagua-Polochic fault zone expose igneous rock and meta-sediments (Fig. 3-10). These igneous rocks are largely felsic and include rhyolites, two mica granites, and granite porphyries (Fig. 3-10). Based on this, the Motagua-Polochic fault zone is identified here as a contributing source for the Toledo formation sandstones.

The Toledo formation contains a high volume percent of carbonate grains (Lc) that were not utilized in the provenance calculation by Dickinson (1985). However, their occurrence warrants mention. Guatemala and Belize hosts extensive Cretaceous carbonate units. The folded and faulted limestone mountains of Guatemala are located just south of the Belize basin along the Motagua-Polochic fault zone and are identified as a contributing source of the carbonate grains for the Toledo formation.

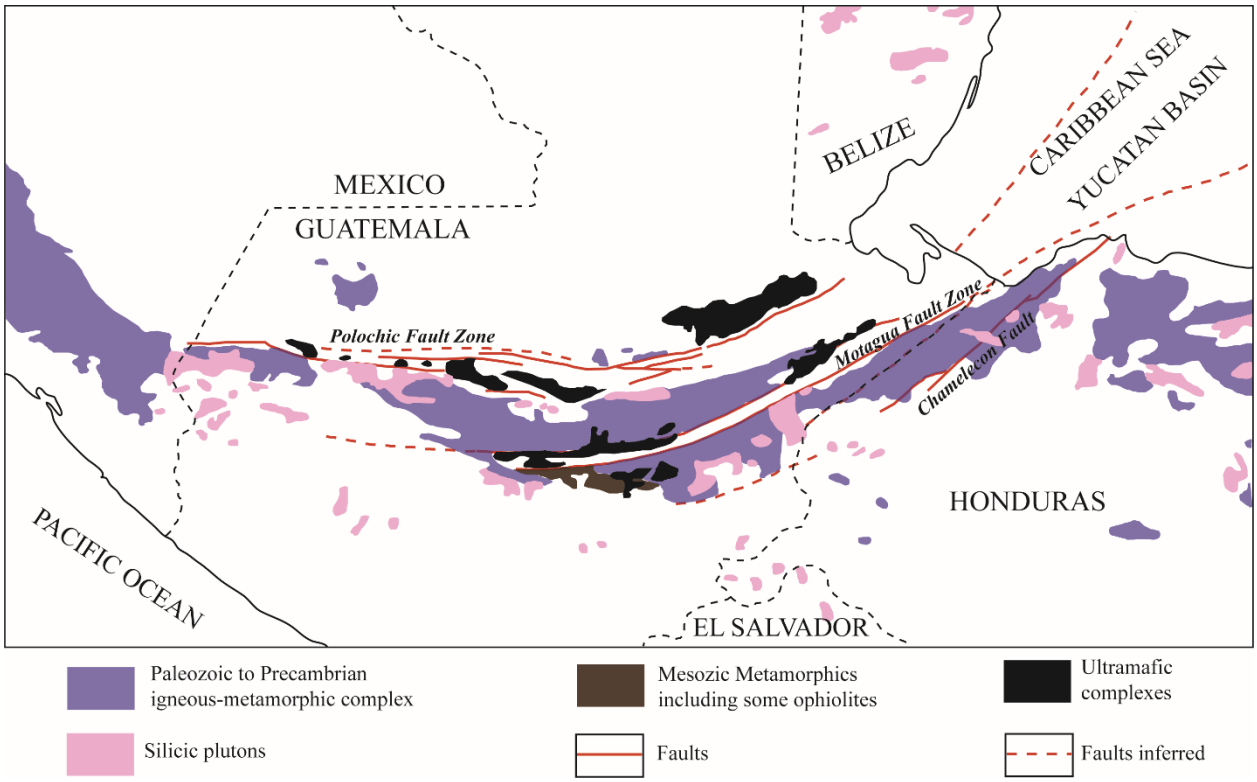

Figure 3-10: Map showing the location of the El Tambor accretionary complex of Guatemala and silicic plutons in southern Belize. After Case (1980).

Conclusion

Petrofacies analysis of wackestones-packestones within the Toledo formation shows a dominance of non-skeletal grains, while skeletal fragments are largely composed of restricted marine assemblages including red algae, gastropods, and foraminifera. The carbonates are interpreted to be deposited in a slope setting based on models of Schlager. The Toledo sandstones are classified as lithic arenites that are texturally submature due to angular to subrounded grains that are poorly to moderately sorted. Compositionally, they are immature due to the dominance of unstable lithic fragments. Diagenetic features include carbonate cement characteristic of marine and meteoric phreatic zones. These features, coupled with the submature nature of the sandstones limits the potential of the sandstones as reservoirs for hydrocarbon or groundwater resources. However, the formation may serve as a seal for Cretaceous reservoirs. The composition of the Toledo sandstones indicates that the provenance area is a recycled orogen related to the collision of the North American and Caribbean tectonic plates.

References

Adams, A.E., MacKenzie, W.S., Guilford, C., 1997, Atlas of sedimentary rocks under the microscope, 104 p.

Bhatia, M.R., 1983, Plate tectonics and geochemical composition of sandstone, Journal of Geology 91, p 611-627.

Boggs, S., Jr., 2006, Principles of Sedimentology and Stratigraphy, Fourth Edition, Pearson Prentice Hall, 688 pp.

Case, J.E., 1980, Crustal setting of mafic and ultramafic rocks and associated ore deposits of the Caribbean region, U.S. Geological Survey Open File report 80-304, 99 p.

Dickinson, W.R., 1985, Interpreting provenance relations from detrital modes of sandstones. *In* Zuffa, G. G (ed.), Provenance of Arenites, p 333-361.

Dickinson, W.R., Beard, L.S., Brakenridge, G.R., Erjavec, J.L., Ferguson, R.C., Inman, K.F., Knepp, R.A., Lindberg, F.A., and Ryberg, P.T., 1983, Provenance of North American Phanerozoic sandstones in relation to tectonic setting. Geol. Soc. Am. Bull. 93, p. 222–235.

Dickinson, W.R., and Suczek, C.A., 1979, Plate tectonics and sandstone compositions, American Association of Petroleum Geologists Bulletin, V. 63, No. 12, p. 2164–2182.

Longman, M. W., 1980, Carbonate diagenetic textures from near surface diagenetic environments: American Association of Petroleum Geologists Bulletin, vol. 64, no. 4, p. 461–487.

Roster, B.P., and Korsch, R.J., 1986, Determination of tectonic setting of sandstone-mudstone suites using SiO2 content and K2O./Na2O ration, Journal of Geology 94, p. 635-650.

Schlager. W., 2005, Carbonate sedimentology and Sequence Stratigraphy, Concepts in Sedimentology and Paleontology 8, Society for Sedimentary Geology (SEPM), 200 pp.

Vinson, G.L., 1962, Upper Cretaceous and Tertiary Stratigraphy of Guatemala: Bulletin of American Association of Petroleum Geologists v. 62, No. 4, p. 425 – 456.

4. PRELIMINARY SOURCE ROCK EVALUATION TOLEDO FORMATION, BELIZE

Jason D. Fisher and David T. King Jr.

Target Journal – *Petroleum Geology*

Abstract

A relative thick early Paleogene sedimentary succession outcrops in the Toledo district of southern Belize, along the new Mile 14 highway (southern Belize) from Belize to Guatemala, which cuts the formation across strike. The informal Toledo formation reaches about 3000 m (~10,000 ft) thickness in exploration wells and consists mainly of calcareous interbedded sandstones and mudstones, with minor conglomerates and carbonates. The informal Toledo formation represents submarine fan deposits and lies conformably/unconformably on Cretaceous limestone and or the 'K/T' boundary.

Based on exploration drilling, the Toledo formation displays good seal potential for the Cretaceous Campus Formation and good source potential for turbiditic beds within the formation. We carried out preliminary analysis of 13 outcrop samples of the Toledo formation using Leco carbon analysis and Rock Eval II Pyrolysis to assess the hydrocarbon potential of this unit. The total organic carbon (TOC) values range from 0.5 – 1.86 wt% and Hydrogen Index values (HI) range from 5 to 77 mg HC/g TOC. Samples from the Toledo formation contain mostly type III/IV kerogen indicating terrigenous organic matter derived from woody plants. The T_{max} values range from 430 to 439 °C. Based on T_{max} and PI values, the samples are immature to early mature in terms of

hydrocarbon generation. Geochemical results of wells drilled in southern Belize found in unpublished reports from the Geology and Petroleum Department of Belize shows very low TOC values, which suggest that the kerogen is primarily oxidized. Though these results are preliminary, they are significant in terms of a regional understanding of the petroleum geochemistry of the Belize basin.

Introduction

Oil and gas exploration in Belize began in the 1930s with over 80 wells drilled to date. Most exploration efforts focused on the northern Corozal basin, where the Spanish Lookout and Never Delay fields were discovered in 2005 and 2009. Wells drilled in southern Belize have encountered encouraging hydrocarbon shows coupled with several oil seeps generally reported in Upper Cretaceous limestones. The most recent well drilled in 2014 by US Capital Energy, Temash #2, was not declared a discovery. Petersen et al. (2012) have carried out source-rock evaluation and organic geochemistry on Upper Cretaceous limestones from the Belize basin. The results identified organically lean source rocks (< 0.5 wt% total organic matter –TOC) and very low S2 pyrolysis yield.

Hydrocarbon potential in the Paleogene deep-water Toledo formation has been identified in the Palmetto Caye 1 well wherein thin organic-rich laminae constitute a significant component of the rock over great thicknesses within the ~10,195 ft of section thus far penetrated offshore (Sanchez-Barreda 1990). There is also potential in the Punta Gorda #1 well based on unpublished reports. Results from unpublished geochemical reports on samples from these wells identified very low organic matter

(less than 0.5 wt % TOC) composed of oxidized terrestrial kerogen. This study attempts to understand/assess the hydrocarbon source potential of the formation at the outcrop level. Geochemical techniques are used to assess the quantity, quality, and thermal maturity of sedimentary organic matter from the perspective of hydrocarbon generation.

Geologic Setting

The Belize basin is a Late Jurassic to Paleogene feature located in southern Belize and is the eastward extension of the Chapayal basin in Guatemala (Vinson, 1962; Bryson, 1975; Kim et al., 2011). Just south of the southern limit of the basin lies the Motagua-Polochic fault system, a left-lateral strike-slip fault system, related to the collision of the North American and Caribbean plates (Fig.4-1). The Cenozoic section of the Belize basin crops out continuously in the south along the northeast section of the Southern highway to the village of Dump (along strike) in the south and to Jalacte village to the northwest (across strike). This section consists largely of the clastic Toledo formation with thicknesses of up to ~ 3000 m (~10,000 ft) observed in exploratory wells. This thick siliciclastic sequence unconformably/conformably overlies Upper Cretaceous carbonates and/or the 'KT' boundary ejecta deposits. Cretaceous and Paleogene sediments, particularly the informal Toledo formation, exhibit substantial thickening over short lateral distances within the basin, thus indicating the presence of faults active since Cretaceous (Bryson, 1975; Whittaker, 1983).

The siliciclastic sequence of the Toledo formation is comprised of interbedded sandstone and mudstone, sandstone, conglomerates, and minor carbonates and is a submarine fan deposit (Fisher and King, 2015, 2016). Fisher and King (2015) divided

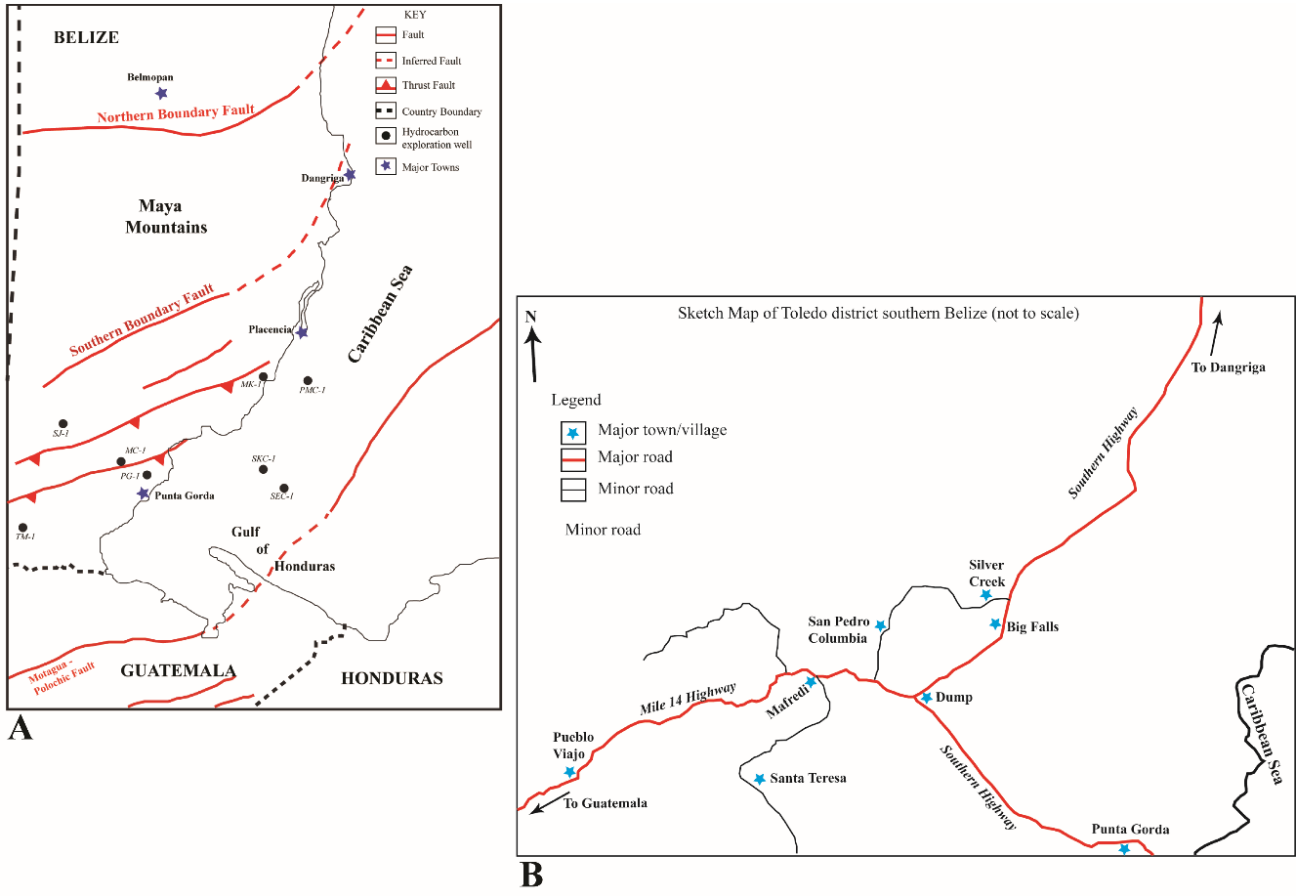

Figure 4-1: Simplified structural map of central and southern Belize showing key faults, major towns, and locations of exploratory wells drilled (modified after Purdy et al., 2003); (B) Sketch map of southern Belize showing highways, roads, and key towns. The study area follows the southern highway to Dump and from Dump to Pueblo Viajo to the west.

the sequence into seven lithofacies (i.e., facies A-G of the submarine fan model of Mutti and Ricci-Lucchi, 1975).

Organic rich unit are observed in facies C, D, and E. Facies C (Fig. 4-2) is fine- to coarse-grained sandstone interbedded with thin layers of mudstone. Sandstone beds

are commonly 0.25 to 2.5 m thick and grading upwards to thin mudstone layers. Sandstone-to-shale ratios are generally high. Beds show little or no channelization as tops and bottoms of beds are parallel. Due to the presence of thin interbeds of mud, sole marks, and trace fossils tend to be well preserved.

Facies D (Fig. 4-3) consists of interbedded thin, calcareous sandstone and silty mudstone. The sandstone is fine to medium grained and contains organic matter in some outcrops. Beds are generally 0.05 to 0.40 m thick, parallel, and persist laterally for great distances. Sandstone-to-mudstone ratios are variable and are usually one or less. Thick facies D strata are transitional with thin facies C beds, and the two are commonly interbedded.

Facies E (Fig. 4-4) deposits are similar to facies D in that they consist of interbedded sandstones and mudstones. However, facies E differs by the occurrence of wavy and discontinuous bedding in sandstones with a high to very high ratio of sandstone to mudstone.

Organic matter throughout these facies and is dispersed in a range particle sizes (Fig. 4-5). Siltstone-mudstone pairs contain disseminated organic matter as well as organic matter concentrated in laminae and trace fossils (Fig. 4-5). In sandstones, the organic matter is typically dispersed. However, zones of concentrated plant macerals occur locally in fine to medium grained sandstones.

Figure 4-2: Facies C. Interbedded mudstone and thin to thick sandstone beds.

Figure 4-3: Facies D. Thinly interbedded sandstone and silty mudstone, showing small channeling.

Figure 4-4: Facies E. Interbedded sandstones and mudstones with sandstones displaying wavy and discontinuous bedding.

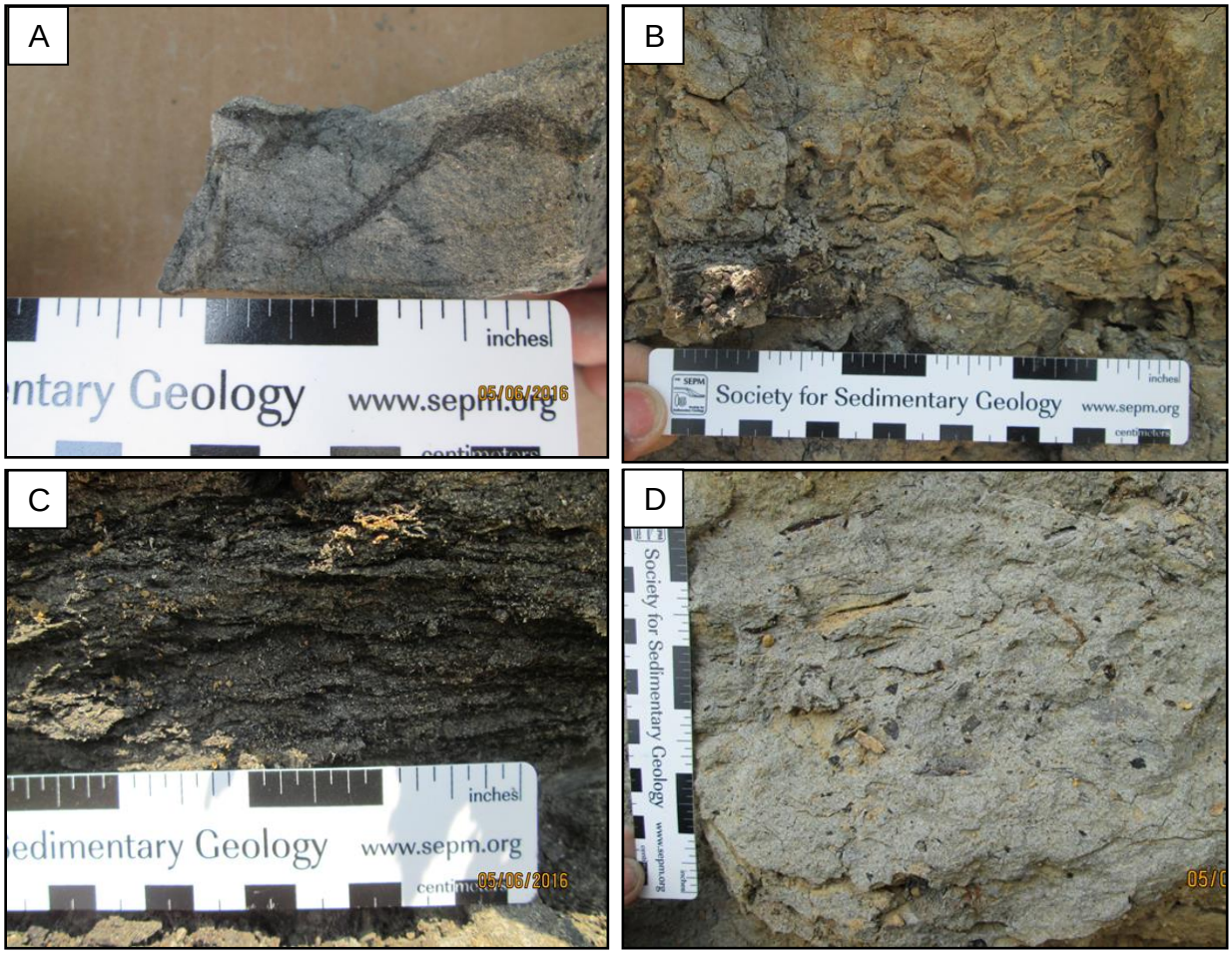

Figure 4-5: Occurrence of organic matter in rock units. (A) Organic matter concentrated in trace fossil. (B) Zone with coarse grained plant macerals. (C) Organic matter concentrated in laminae. (D) Zone of medium grained plant macerals.

Materials and Methods

Geochemical analyses were carried out on 13 samples of siltstones/fine sandstones, silty mudstones, and sandstones containing organic matter described in the previous section. These were collected from outcrops along the Mile 14 highway in the Belize basin, southern Belize, during the summer 2016 field session. LECO total organic carbon (TOC) analysis and Rock Eval II Pyrolysis were used to determine source rock parameters, including type and amount of organic matter (OM), thermal maturity, and hydrocarbon generation potential. The carbonate content of each sample was also determined. Intertek Westport Technology, Houston, Texas, completed these geochemical analyses.

About 15 g of each sample was grinded and homogenized before analysis. For Leco TOC analysis, powdered aliquots of the samples were chemically treated using hydrochloric acid for 12 to 24 h to remove carbonates. Once dissolution of carbonates was complete, samples were washed and analyzed for carbon content on a LECO carbon analyzer. Rock Eval II pyrolysis was carried out on powdered aliquots of the samples. The samples are progressively heated from 300 to 550 °C in the absence of oxygen, leading to the release of hydrocarbon and carbon dioxide.

The quantity of organic matter, total organic carbon (TOC), is measured in weight percent. Very poor source rocks have TOC values below 0.5 (wt %); poor source rocks ranges from 0.5 to 1 (wt %); fair source rocks have TOC values ranging from 1 to 2 (wt %); good source rocks have TOC values ranging from 2 to 4 (wt%); very good source

rocks have TOC values ranging from 4 to 12; and excellent source rocks have TOC values of > 12 (wt%) (McCarthy et al. 2011).

The quality of organic matter is assessed using S1, S2, and S3, obtained from pyrolysis data. S1 is the release of free hydrocarbons at about 300 °C; S2 is the percentage of the cracked hydrocarbons during pyrolysis at maximum temperature T_{max}, whereas S3 is the release of organically bound CO_2 at temperatures ranging from 300 to 550 °C. Hydrogen and oxygen indices (HI and OI) are determined from TOC and Rock-Eval Pyrolysis data, where HI and OI are equivalent to H/C and O/C ratios in the kerogen, respectively. The production index (PI) is equal to S1/(S1 + S2). The potential yield (PY) = (S1 + S2) is an important parameters in assessing the source potential.

Thermal maturity of organic matter is typically assessed using vitrinite reflectance (Ro) and T_{max} values obtained from Rock Eval pyrolysis. For this study only T_{max} values are reported.

Results and Discussion

Quantity and Quality of organic matter

The organic richness of sedimentary rocks is important in the assessment of sediments as a source for hydrocarbons. The results for all analyzed samples are in Table 4-1. The analyzed samples contain TOC values from 0.2 to 1.86 wt% indicating poor to fair source rocks.

Genetic type of organic matter

The initial type of organic matter of a source rock is essential for the prediction of the source rock's hydrocarbon potential. Hydrogen indices (HI) values and S2/S3 have been used to indicate different organic matter types and the main hydrocarbon products generated (Peters and Cassa, 1994; Table 4-2). Results from the analysis (Table 4-1) show low hydrogen indices values ranging from 4 to 77 mg HC/g TOC and low S2/S3 values from 0.25 to 3.89. This indicates that the samples contain type III/IV kerogen. Type III kerogen is gas prone and type IV kerogen is commonly referred to as dead carbon that generates little to no hydrocarbons (Peters and Cassa, 1994).

Based on pyrolysis data kerogen classification diagrams (Van Krevlen plots) using hydrogen and oxygen indices (Fig. 4-5), the Toledo samples contain type IV kerogen marginally grading to type III. This agrees with the classification scheme using HI and S2/S3 described by Peters and Cassa (1994). Plots of HI versus T_{max} and S2 versus TOC (Figures 4-7 and 4-8) agree with the HI and S2/S3 classification and the modified Van Krevlen plot.

Eighty-five percent of the samples are classified a type IV kerogen, which may represent organic matter affected by weathering or oxidization of the outcrops or represent recycled organic matter. The organic matter appears to be from terrestrial source as confirmed by the kerogen type and woody organic fragments observed in outcrops. The hydrocarbon potential (S1 + S2) is generally very low. The presence of boring bivalve (or "shipworm") ichnofossils (i.e., *Teredolites sp.*) in terrestrial wood fragment suggests transportation from a shallow locality in close proximity (Figure 4-9).

Table 4-1: Rock Eval Pyrolysis and LECO TOC data for samples of the Toledo formation

Sample ID	Rock Type	Carbonate content % wt.	SOURCE QUALITY								THERMAL MATURITY	
			TOC	S_1	S_2	S_3	$S_1 + S_2$	S_2/S_3	HI	OI	PI	T_{max}
FTD48A	Siltstone	44.57	0.26	0.07	0.08	0.28	0.15	0.29	31	108	0.47	0
FTD75B	Siltstone	38.45	0.38	0.02	0.08	0.14	0.04	0.57	5	37	0.5	0
FTD75C	Siltstone/f. sandstone	34.64	0.29	0.02	0.04	0.12	0.06	0.33	14	42	0.3	0
FTD76B	Mudstone/siltstone	30.89	0.49	0.02	0.11	0.13	0.13	0.85	22	26	0.15	0
FTD77A	Siltstone	33.53	1.22	0.05	0.28	0.21	0.33	1.33	23	17	0.15	439
FTD77D	Siltstone	42.3	0.71	0.06	0.26	0.22	0.32	1.18	37	31	0.19	436
FTD78B	Siltstone	39.54	1.86	0.05	0.87	0.32	0.92	2.72	47	17	0.05	432
FTD78C	Siltstone	24.49	1.68	0.05	1.3	0.34	1.35	3.82	77	20	0.04	430
FTD79A	Siltstone/f. sandstone	36.35	1.35	0.02	0.87	0.46	0.89	1.89	64	34	0.02	434
FTD79B	Siltstone	36.5	0.38	0.05	0.07	0.23	0.12	0.30	18	60	0.42	0
FTD79C	Siltstone/ f. sandstone	63.62	1.07	0.05	0.5	0.3	0.55	1.67	47	28	0.09	432
FTD79F	Siltstone/ f. sandstone	36.31	0.42	0.05	0.11	0.17	0.16	0.65	26	41	0.31	0
FTD80B	Sandstone	33.24	0.91	0.05	0.04	0.16	0.09	0.25	4	18	0.56	0

Table 4-2: Geochemical parameters describing kerogen type (quality) and character of products modified after Peters and Cassa (1994).

Kerogen Type	HI (mg HC/g TOC)	S_2/S_3	Expelled product at maturity
I	> 600	> 15	Oil
II	300-600	10-15	Oil
II/III	200-300	5-10	Mixed oil and gas
III	50-200	1-5	Gas
IV	< 50	< 1	None

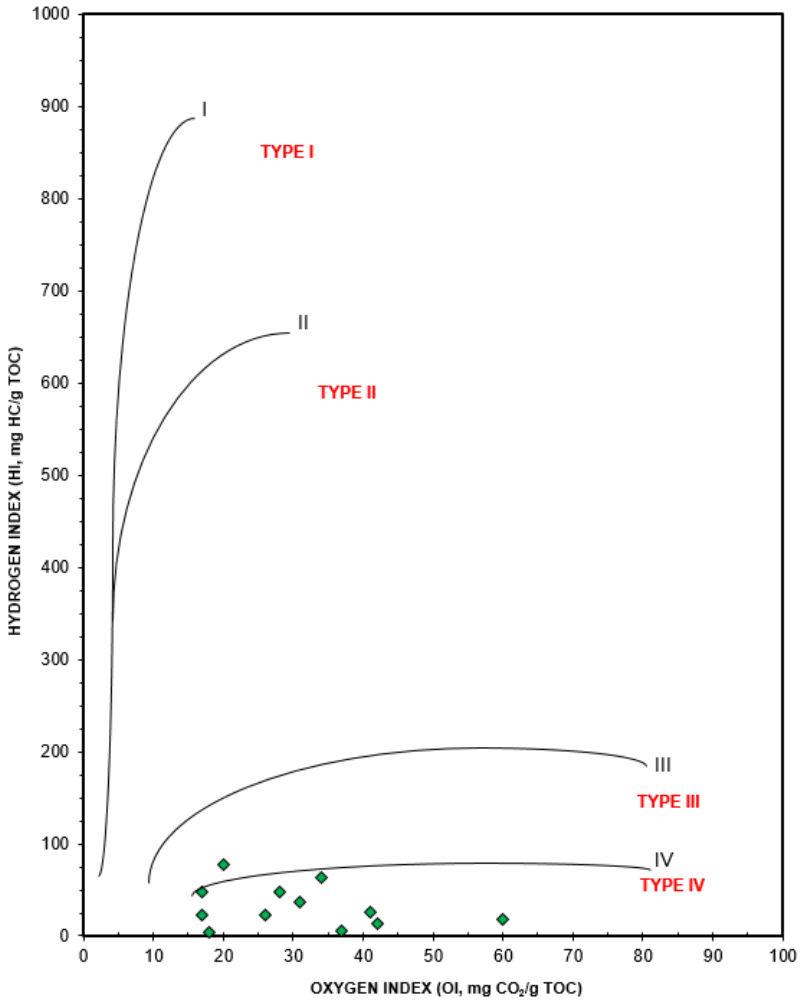

Figure 4-6: Modified van Krevlen plot for the Toledo formation.

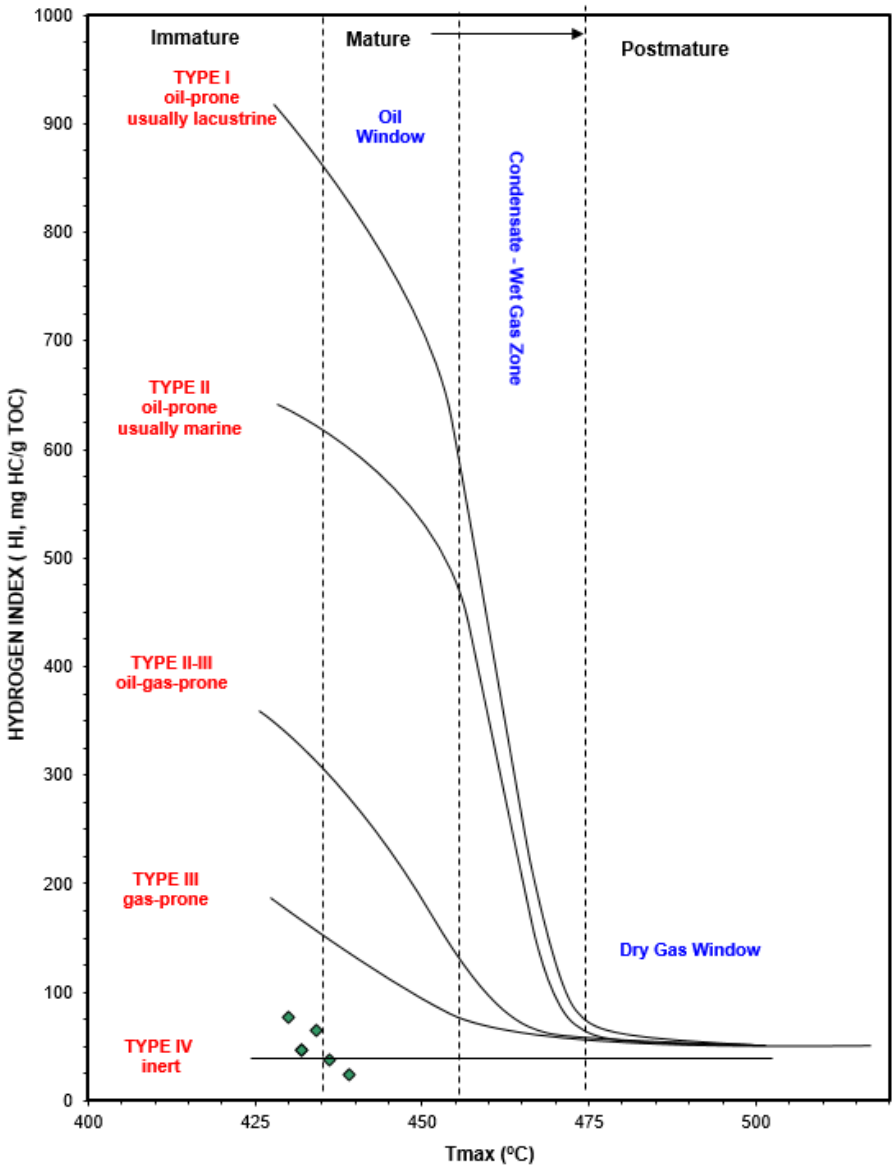

Figure 4-7: Kerogen type and maturation based on T_{max} and Hydrogen Index (HI).

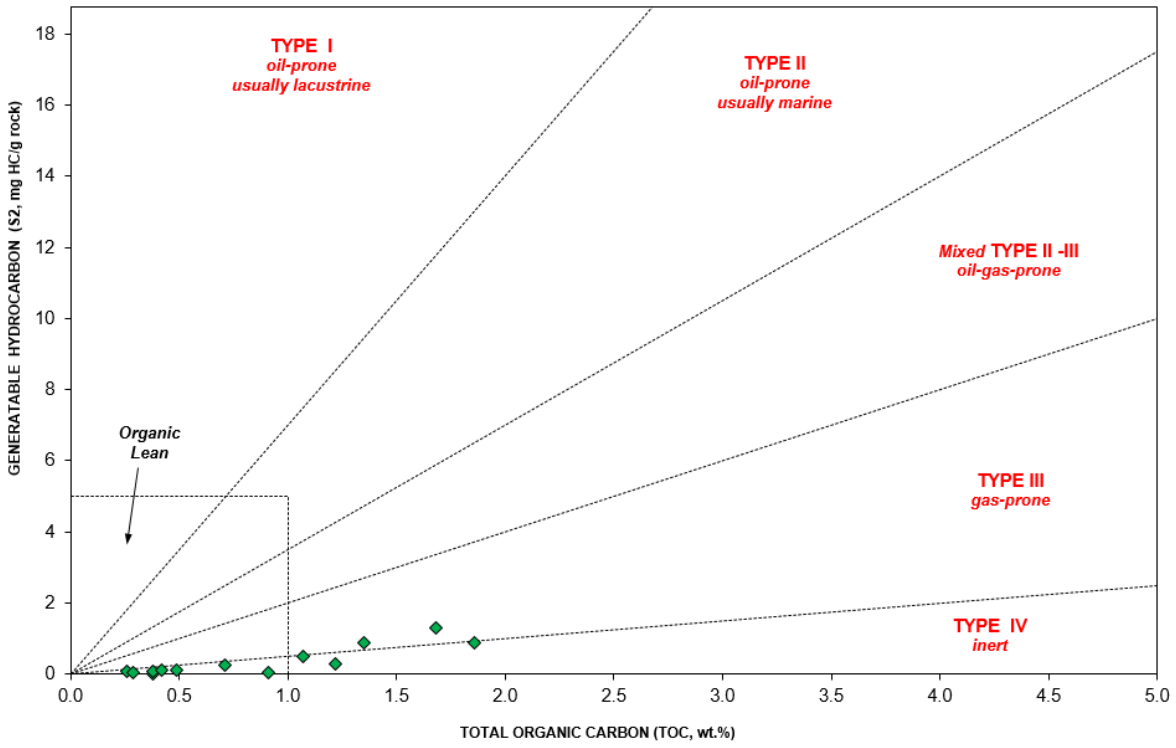

Figure 4-8: Plot of kerogen type based on TOC and S2 values.

Figure 4-9: Boring bivalve ichnofossil *Teredolites* sp. in terrestrial wood fragment.

Kerogen maturity

The concentration and distribution of hydrocarbons within a source rock depend on the type of organic matter and its degree of thermal alteration or its maturity (Tissot and Welte, 1984). In this study, the pyrolysis T_{max} values generally are unreliable due to poor S2 response. Only 50% of the samples provided results for T_{max} giving temperatures of 430 - 439°C. Based on the kerogen classification diagram constructed using HI versus T_{max} (Figure 4-6), the results suggests that these rocks are immature to mature.

Conclusions and Recommendations

Thirteen outcrop samples were collected in southern Belize in order to carry out preliminary investigations on the organic-rich submarine fan facies of the Paleogene Toledo formation along the Mile 14 highway in southern Belize. Rock-Eval parameters and total organic carbon were determined in order to evaluate the Toledo formation as a potential source rock.

The analyses show that the Toledo formation rocks are fair to poor source rocks (TOC values ranging from 0.2 to 1.86 wt %) with kerogen of type III/IV inferred from low hydrogen indices (4 to 77 mg HC/TOC), S2/S3 (< 1 to 3.82) values, and S2 versus TOC plot. Results show that outcrop based samples have generally low hydrocarbon potential. The rocks sampled are immature to mature and are gas-prone. Their status according to PI versus T_{max} plot indicates a low position in the oil window.

To better assess the hydrocarbon potential of the formation it is recommended that a geochemical log of the Palmetto Caye-1 and Punta Gorda-1 wells be conducted.

This would involve collecting closely spaced samples allowing for the critical evaluation of potential source intervals using Rock Eval pyrolysis and total organic carbon data supplemented with vitrinite reflectance.

Acknowledgments

This research is funded in part by the Big Creek Group, Independence, Belize. We are most grateful for their support of research on Belize geological history. The American Association of Petroleum Geologists (AAPG), Geological Society of America (GSA), and the Waters-Folse research grant from the Department of Geosciences, Auburn University, AL, provided additional funding. In addition, J.F. thanks Gerald Westby for accompanying him into the field area. We also thank Dr. Chuck Savrda, Ichnologist, for identification of the trace fossil *Teredolites* sp.

References

Bryson, R.S., 1975, Regional Geology, Petroleum and Mineral Potential of southern Belize: Denver, Colorado, Anschutz Overseas Corporation, 22p.

Fisher, J. D., and King, Jr., D. T, 2016, Early Tertiary submarine fan deposits in southern Belize: Gulf Coast Association of Geological Societies Transactions, v. 66, p. 107–123.

Fisher, J. D., and King, Jr., D. T., 2015, Stratigraphy of the Toledo formation, Belize basin, southern Belize: Gulf Coast Association of Geological Societies Transactions, v. 65, p. 107–123.

Kim, Y., Clayton, R.W., Keppie, C., 2011, Evidence of a collision between the Yucatán block and Mexico during Miocene: Geophysical Journal International, v. 187, p. 989-1000.

McCarthy, K., Rojas, K., Niemann, M., Palmowski, D., Peters, K., Stankiewicz, A., 2011, Basic Petroleum Geochemistry for source rock evaluation, Oilfield Review Schlumberger, V. 23, no. 2, p. 32 – 43.

Mutti, E., and Ricci Lucchi, F., 1972, Le torbiditi dell|Apennino Settentrionale Introduzione all|analisi di facies: Memorie. Soc. Geoligica Italiana 11, 161-199.

Mutti, E., and Ricci Lucchi, F.,1975, Turbidite facies and facies associations. *In* Mutti E. et al. (eds.), Turbidite facies and facies associations in some selected formations of northern Apennines: IAS International Congress "Nice '75", Exc. Guidebook A-11, p. 21-36.

Peters, K.E., and Cassa, M.R., 1994, Applied source rock geochemistry, in Magoon, L.B., and Dow, W.G., eds., The petroleum system—From source to trap: Tulsa, Okla., American Association of Petroleum Geologists Memoir 60, p. 93-117.

Petersen, H.I., Holland, B., Nytoft, H.P., Cho, A., Piasecki, S., de la Cruz, J., and Cornec, J.H., 2012, Geochemistry of crude oils, seepage oils and source rocks from Belize and Guatemala: indications of carbonate-sourced petroleum systems: Journal of Petroleum Geology, v. 35, p.127-163.

Sanchez-Barreda, Luis, A., 1990, Why wells have failed in southern Belize: Oil and Gas Journal, August, p. 97-103.

Tissot, B.P., and Welte, D.H., 1984, Petroleum Formation and Occurrence, second edition, Springer, New York, 699p.

Vinson, G., 1962. Upper Cretaceous and Tertiary Stratigraphy of Guatemala: Bulletin of American Association of Petroleum Geologists v. 62, No. 4, p. 425 – 456.

Whittaker, R. C., 1983. The Hydrocarbon potential of Belize, Unpublished Master's Thesis: London, Department of Geology, Imperial College.

5. SUMMARY

Published literature of the informal Toledo formation focuses on the description of Toledo equivalent strata in southern Guatemala and to a lesser extent on the equivalents in Belize with even more limited knowledge of its depositional environment. The formation has been identified as a 'flysch sequence' (Schafhuser et al., 2003) and has been described as a sequence of limestone, sandstone, and shales that are thin, regular, and interbedded deposited in geosyncline/foredeep shortly before a major orogeny. Key findings of the project includes: (1) recognition of seven lithofacies at outcrop scale; (2) recognition of a sub-marine fan complex setting for the Toledo formation; (3) classification of the sandstones as immature-submature lithic-arenites; (4) poor reservoir quality, but good seal potential of the sandstones; (5) Motagua-Polochic fault zone region as the source for the Toledo formation sandstones; and (6) fair to poor source rock potential of the organic rich facies.

The present study documents that the Toledo formation occurs as sub-marine fan deposits with seven major lithofacies, with sandstones being the dominant lithology. These are interpreted as channelized and non-channelized deposits sub-marine fan complex deposits and were deposited by gravity and grain flow processes. Three major depositional units/architectural elements have been identified, channel, lobe, and sheet sands. Four major fan associations were identified: (1) Outer fan/depositional lobe deposits; (2) Mid-fan deposits; (3) Submarine canyon deposits; and (4) Shelf-derived deposits (carbonates).

Petrographic analysis of the shelf derived carbonate samples from the Toledo formation are dominated by reworked carbonate lithic grains of various sizes. The skeletal grains are dominated by shallow water benthics particularly algae, mollusks, and foraminifera (both benthic and planktic). The limestones can be interpreted as slope deposits based on models described by Schlager (2005).

Sandstones, the dominant lithology in the Toledo formation, are classified as submature lithic-arenites. The lithic grains are dominated by carbonates followed by a variety of igneous grains. Calcite cementation is prolific in the sandstones, occluding pore spaces, and is consistent with diagenesis in marine and meteoric phreatic zones.

Plots of the detrital modes of the Toledo formation's sandstones based on ternary diagrams from Dickinson (1985) identified a recycled orogen provenance. Orogenic recycling occurs in different tectonic settings where rocks are deformed, uplifted, and eroded. Based on the regional setting of the basin, the Motagua-Polochic fault region is the likely source terrain. The region consists of a suite of igneous (ultramafic, mafic, and silicic), sedimentary, and meta-sedimentary rocks. The ultramafic and mafic igneous rocks, the El Tambor complex, is an accretionary complex formed during the collision of the North American and Caribbean Plate boundaries along the Motagua-Polochic fault system. The complex is located just south of the Belize basin and is inferred as the source of the igneous rocks in the Toledo sandstones. The silicic igneous rocks occur as plutons and include rhyolites, two-mica granites, and granite porphyries. The dominance of monocrystalline over polycrystalline quartz suggests contribution from a granitic source, herein identified as

these silicic plutons occurring along the fault system. The sedimentary rocks are carbonates of the Yucatán platform exposed in outcrops of the folded and faulted mountains in southern Guatemala, just south of the Belize basin. These are identified as a contributing source of the large volume percent of carbonate grains in the sandstones.

The Toledo formation has been identified as a major part of the Upper Cretaceous to Paleogene lower aquifer system in southern Belize and has demonstrated hydrocarbon source/seal potential onshore and offshore. Results from the study show porosity occlusion in the sandstones coupled with poor to moderate sorting (texturally submature), which reduces its reservoir potential whether for hydrocarbon or groundwater resources. On the other hand, there is good seal potential due to the formation's extensive thickness, large scale interbeds of mudstone and sandstone, as well as the porosity occlusion. There is also the stratigraphic trapping potential as a diagenetic barrier.

Preliminary assessment of the hydrocarbon source-rock potential of the organic rich facies of the formation was carried out. Results show that the Toledo formation rocks are fair to poor source rocks (TOC values ranging from 0.2 to 1.86 wt %) with kerogen of type III/IV inferred from low hydrogen indices (4 to 77 mg HC/TOC), S2/S3 (< 1 to 3.82) values, and S2 versus TOC plot. The rocks sampled have generally low hydrocarbon potential are immature to mature and are gas-prone. According to PI versus T_{max} plot, the samples have a low position in the oil window.

6. COMBINED REFERENCES

Adams, A.E., MacKenzie, W.S., and Guilford, C., 1997, Atlas of sedimentary rocks under the microscope, 104 p.

Bhatia, M.R., 1983, Plate tectonics and geochemical composition of sandstone, Journal of Geology 91, p 611-627.

Boggs, S., Jr., 2006, Principles of Sedimentology and Stratigraphy, Fourth Edition, Pearson Prentice Hall, 688 pp.

Browne, G. H., Slatt, R.M., and King, P.R., 2000, Contrasting styles of basin-floor fan and slope fan deposition: Mount Messenger Formation, New Zealand. *In* Bouma, A.H., and Stone, C.G. (eds.), Fine-grained turbidite systems: Tulsa, Oklahoma, AAPG Memoir 72 and SEPM Special Publication 68, p. 143-152.

Bryson, R.S., 1975, Regional Geology, Petroleum and Mineral Potential of southern Belize: Denver, Colorado, Anschutz Overseas Corporation, 22 p.

Burne, R.V., 1995, The return of “The Fan that never was”: Wesphalian turbidite systems in the Variscan Culm Basin: Bude Formation (southwest England). *In* Plint, A.G., (ed.) Sedimentary Facies Analysis: A tribute to the research and teaching of Harold G. Reading, International Association of Sedimentologists Special Publication 22, p. 101-135.

Case, J.E., 1980, Crustal setting of mafic and ultramafic rocks and associated ore deposits of the Caribbean region, U.S. Geological Survey Open File report 80-304, 99 p.

Cornec, J.H., 2003, Geology map of Belize, 1:750,000: Belmopan, Belize, Geology and Petroleum Office.

de V. Wickens, H., and Bouma, A.H., 2000, The Tanqua fan complex, Karoo Basin, South Africa—Outcrop analog for fine-grained, deepwater deposits. *In* Bouma, A.H. and Stone, C.G. (eds.), Fine-grained turbidite systems: Tulsa, Oklahoma, AAPG Memoir 72 and SEPM Special Publication 68, p. 153-164.

Dickinson, W.R. and Suczek, C.A., 1979, Plate tectonics and sandstone compositions, American Association of Petroleum Geologists Bulletin, V. 63, No. 12, p. 2164–2182.

Dickinson, W.R., 1985, Interpreting provenance relations from detrital modes of sandstones. *In* Zuffa, G. G (ed.), Provenance of Arenites, p. 333-361.

Dickinson, W.R.; Beard, L.S.; Brakenridge, G.R.; Erjavec, J.L.; Ferguson, R.C.; Inman, K.F.; Knepp, R.A.; Lindberg, F.A.; Ryberg, P.T, 1983, Provenance of North American Phanerozoic sandstones in relation to tectonic setting. Geological Society of America Bulletin, v. 93, 222–235.

Dixon, C.G., 1956, Geology of Southern British Honduras with notes on adjacent areas: Belize City, British Honduras, Government Printing Office, p. 1-85.

Fisher, J. D., and King, Jr., D. T., 2015, Stratigraphy of the Toledo formation, Belize basin, southern Belize: Gulf Coast Association of Geological Societies Transactions, v. 65, p. 107–123.

Fisher, J. D., King, D. T., Jr., and Da Gama, R. O. B. P., 2016, Submarine fan complex facies of the Paleogene Toledo formation in southern Belize: Boulder, Geological Society of America Abstracts with Programs, v. 48, no. 3, Abstract 28–1.

Geology and Petroleum Department, Ministry of Energy, Science, Technology and Public Utilities, Government of Belize, 2014, Geophysical Surveys and wells drilled in Belize 2000-2014, map.

GEOMEDIA, 2014, Assessment of Groundwater Resources in the southern Coastal Water Province of Belize referred to as Savannah Groundwater Province, unpublished, final report: United Nations Development Programme (UNDP), Belmopan, Belize, GCCA/PS/2013/14, p.136.

Keller, G., Stinnesbeck, W., Adatte, T., Holland, B., Stüben, D., Harting, M., de Leon,C., and de la Cruz, J., 2003, Spherule deposits in Cretaceous-Tertiary boundary sediments in Belize and Guatemala: Journal of the Geological Society, v. 160, p. 783-795.

Kim, Y., Clayton, R.W., Keppie, C., 2011, Evidence of a collision between the Yucatán block and Mexico during Miocene: Geophysical Journal International, v. 187, p. 989-1000.

King, D.T., Jr., Pope, K.O., and Petruny, L.W., 2004, Stratigraphy of Belize, north of the 17th parallel: Gulf Coast Association of Geological Societies Transactions, v. 54, p. 289-304.

Lallement, H.G., and Gordon M.B., 1999, Deformation History of Roatán Island: Implications for the Origin of the Tela basin (Honduras). *In* Mann, P. (Series

Editor K.J. Hsü), Caribbean basins: Sedimentary basins of the World, 4, p.197-218.

Leroy, S., Mauffret, A., Patriat, P., and Mercier de Lépinay, B., 2000, An alternative interpretation of the Cayman trough evolution from reidentification of magnetic anomalies: Geophysical Journal International, v. 141, p. 538-557.

Link, M.H., and Weimer, P., 1991, Seismic facies and sedimentary processes of submarine fans and turbidite systems: an overview. *In* Weimer, P., and Link, M.H., eds., Seismic facies and sedimentary processes of submarine fans and turbidite systems: New York, Springer-Verlag, p. 3-7.

Lowe, D. R., 1982, Sediment gravity flows: II. Depositional models with special reference to the deposits of high density turbidity currents: Journal of Sedimentary Petrology, v. 52, p. 279–297.

Mattern, F., 2005, Ancient sand rich submarine fans: depositional systems, models, identification, and analysis: Earth-Science reviews, v. 70, p. 167-202.

Mulder, T., and Alexander, J., 2001, The physical character of subaqueous sedimentary density flows and their deposits: Sedimentology, v. 48, p. 269-299.

Mutti, E., and Normark. W.R., 1987, Comparing examples of modern and ancient turbidite systems: problems and concepts. *In* Leggett, J.K. and Zuffa, G.G., (eds.), Marine clastic sedimentology: concepts and case studies: London, Graham and Troutman, p. 1–38.

Mutti, E., and Ricci Lucchi, F., 1972, Le torbiditi dell|Apennino Settentrionale Introduzione all|analisi di facies: Memorie. Soc. Geoligica Italiana 11, p.161-199

Mutti, E., and Ricci Lucchi, F., 1975, Turbidite facies and facies associations. *In* Mutti E. et al. (eds.), Turbidite facies and facies associations in some selected formations of northern Apennines: IAS International Congress "Nice '75", Exc.Guidebook A-11, p. 21-36.

Mutti. E., and Normark, W.R., 1991 An integrated approach to the study of turbidite systems. In Weimer, P. and Link , M.H. (eds.), Seismic facies and sedimentary processes of submarine fans and turbidite systems, Springer, New York, p. 75–106.

NACSN (North American Commission on Stratigraphic Nomenclature), 2005, North American Stratigraphic Code: American Association of Petroleum Geologists Bulletin, v. 89, p. 1547-1591.

Ower, L.H., 1928, Geology of British Honduras: Journal of Geology, v. 36, p. 494-509.

Petersen, H.I., Holland, B., Nytoft, H.P., Cho, A., Piasecki, S., de la Cruz, J., and Cornec, J.H., 2012, Geochemistry of crude oils, seepage oils and source rocks from Belize and Guatemala: indications of carbonate-sourced petroleum systems: Journal of Petroleum Geology, v. 35, p.127-163.

Pickering, K.T., and Corregidor, J., 2005, Mass-transport complexes (MTCs) and tectonic control on basin floor submarine fans, middle Eocene, south Spanish Pyrenees: Journal of Sedimentary Research, v. 75, p. 761-783.

Purdy, E.G., Gischler, E., and Lomando, A.J., 2003, The Belize margin revisited, 2-Origin of Holocene antecedent topography: International Journal of Earth Sciences v. 92, No. 4, p. 552-572.

Ramanathan, R., 1985, Foraminiferal micropaleontological report on Dangriga well-1, offshore Belize: Belmopan, Belize, Geology and Petroleum Office, unpublished report UNDP/BZE/ 83/001, 13 p.

Ramanathan, R., 1990, Foraminiferal micropaleontological report on Belize: Belmopan, Belize, Geology and Petroleum Office, unpublished report UNDP/BZE/ 87/003, 23 p.

Ramanthan, R. and Garcia, E., 1991, Cretaceous paleogeography, foraminiferal biostratigraphy, and paleoecology of Belize basin: Transactions of the 2nd Geological Conference of the Geological Society of Trinidad and Tobago: Port of Spain, Trinidad, p. 203-211.

Reading, H.G., and Richards, M., 1994, Turbidite systems in deep-water basin margins classified by grain size and feeder system: American Association of Petroleum Geologists Bulletin, v. 78, p. 792-822.

Ricci Lucchi, F., 1975a, Depositional cycles in two turbidite formations of northern Apennines: Journal of Sedimentary Petrology, v. 45, p. 1-43.

Ricci Lucchi, F., 1975b, Miocene paleogeography and basin analysis in the Periadriatic Apennines, in H.S. Coy (editor), Geology of Italy, Earth Science Society of Libyan Arab Republic, Tripoli, p. 5-111.

Roster, B.P., and Korsch, R.J., 1986, Determination of tectonic setting of sandstone-mudstone suites using SiO2 content and K2O./Na2O ration, Journal of Geology 94, p 635-650.

Salvador, A., ed., 1994, International Stratigraphic Guide, 2nd ed: International Union of Geological Sciences and Geological Society of America, 214p.

Sanchez-Barreda, Luis, A., 1990, Why wells have failed in southern Belize: Oil and Gas Journal, August, p. 97-103.

Schafhauser, A., Stinnesbeck, W., Holland, B., Adatte, T., and Remane, J., 2003, Lower Cretaceous Pelagic Limestones in Southern Belize: Proto-Caribbean deposits on the Southeastern Maya Block. *In* Bartolini, C., Buffler, R.T., and Blickwede, J., The Circum-Gulf of Mexico and the Caribbean: Hydrocarbon habitats, basin formation, and plate tectonics: Tulsa, Oklahoma, American Association of Petroleum Geologists Memoir 79, p. 624-637.

Schlager. W., 2005, Carbonate sedimentology and Sequence Stratigraphy, Concepts in Sedimentology and Paleontology 8, Society for Sedimentary Geology (SEPM), 200p.

Scholle, P.A., and Spearing, D., 1982, Sandstone depositional environments: American Association of Petroleum Geologists, 410 p.

Shanmugam, G., 2000, 50 years of the turbidite paradigm (1950s–1990s): deep-water processes and facies models—a critical perspective: Marine and Petroleum Geology, v. 17, p. 285-342.

Shanmugam, G., and Moiloa, R.J., 1985, Submarine Fan Models: Problems and solutions. *In* Bouma, A.H., Normark, W.R., and Barnes, N.E., (eds.), Submarine fans and related turbidite systems: New York, Springer-Verlag, p. 29-34.

Shanmugan, G., and Moiola, R.J., 1988, Submarine Fans: Characteristics, Models, Classification and Reservoir potential; Earth Science Review, v 24, p. 383 -428.

Sprague, A. R., Sullivan M. D., Campion K. M., Jensen, G. N., Goulding, F. J., Garfield T. R., Sickafoose, D. K., Rossen, C., Jennette, D. C., Beaubouef , R. T., Abreu V., Ardill, J., Porter, M. L., and Zelt, F. B., 2002a, The physical stratigraphy of deep- water strata: A hierarchical approach to the analysis of genetically related elements for improved reservoir prediction, (Abstract): American Association of Petroleum Geologists Search and Discovery Article 90007, Tulsa, Oklahoma, <http://www.searchanddiscovery.com/abstracts/pdf/2002/annual/SHORT/ndx_41753.pdf> Last accessed August 4, 2014.

Sprague, A. R., Patterson, P. E., Hill, R.E., Jones, C.R., Campion, K. M., Van Wagoner, J.C., Sullivan, M. D., Larue, D.K., Feldman, H.R., Demko, T.M., Wellner, R.W., Geslin, J.K., 2002b, The physical stratigraphy of fluvial strata: A hierarchical approach to the analysis of genetically related stratigraphic elements for improved reservoir prediction, (Abstract): American Association of Petroleum Geologists Search and Discovery Article 90007, Tulsa, Oklahoma, <http://www.searchanddiscovery.com/abstracts/pdf/2002/annual/SHORT/ndx_41780.pdf> Last accessed August 4, 2014.

Stelting, C.E., Bouma, A.H., and Stone, C.G., 2000, Fine-grained turbidite systems: Overview. *In* Bouma, A.H. and Stone, C.G., (eds.), Fine-Grained turbidite Systems: Tulsa, Oklahoma, American Association of Petroleum Geologists Memoir 72, SEPM Special Publication No. 68, p.1-8.

Stow, D.A.V, and Mayall, M., 2000, Deep-water sedimentary systems: New models for the 21st century: Marine and Petroleum Geology, v. 17, p. 125-135. PII: S0264-8172(99)00064-1.

Stow, D.A.V., 1985, Deep-sea clastics: where are we and where are we going? *In* Brenchley, P.J. and Williams, B.P.J., (eds), Sedimentology: Recent Developments and Applied Aspects, Special Publication Geological Society of London, v. 18, p. 67–93.

Vinson, G., 1962. Upper Cretaceous and Tertiary Stratigraphy of Guatemala: Bulletin of American Association of Petroleum Geologists v. 62, no. 4, p. 425 – 456.

Walker, R.G., 1992, Turbidites and submarine fans. *In* Walker, R.G., and James, N.P., (eds.), Facies models; response to sea level change: Toronto, Geological Association of Canada, p. 239-263.

Walker, R.G., and Mutti, E., 1973, Turbidite facies and facies associations, *In* Turbidites and Deep-water sedimentation: Pacific Section, Society of Economic Paleontology and Mineralogy, p. 119-157.

Whittaker, R. C., 1983. The Hydrocarbon potential of Belize, Unpublished Master's Thesis: London, Department of Geology, Imperial College.

Winn, R.D., and Dott, R.H., 1979, Deep-water fan-channel conglomerates of Late Cretaceous age, southern Chile: Sedimentology, v. 26, p. 203-228.